RDU1703313

MACHINABILITY STUDY OF STRUCTURAL AUTOMOTIVE ALLOYS USING ABRASIVE WATERJET MACHINING PROCESS

MOHD AZMIR MOHD AZHARI

IZWAN BIN ISMAIL

MEBRAHITOM ASMELASH GEBREMARIAM

MD. MUSTAFIZUR RAHMAN

NURRINA BINTI ROSLI

RESEARCH VOTE NO.:

RDU1703313

Fakulti Teknologi Kejuruteraan Pembuatan dan Mekatronik

2019

ACKNOWLEDGEMENT

Authors would like to gratefully acknowledge the financial support from the Universiti Malaysia Pahang through RDU1703313.

ABSTRACT

The need of cleaning automotive paint without secondary pollution has recently become a major concern globally. The waterjet technology has extended its application to include surface treatment, machining, cleaning and cutting of materials. Plain waterjet is frequently used for cleaning since its offers environmentally friendly concept which results near zero pollution to the surroundings. The present work aims to analyse and optimise the use of multiple passes in waterjet cleaning process for removal of automotive paint using response surface methodology (RSM) approach. The effect of surface roughness (R_a) and its topography were analysed. RSM, analysis of variance (ANOVA), fractional factorial at 2-levels and central composite design (CCD) were utilized to optimize the plain waterjet process parameters for effective cleaning of paint. It was observed that the lateral feed and pressure were the most significant control factors in influencing the cleaning performance criteria. A mathematical model was developed using linear regression analysis to predict the R_a in terms of cleaning parameters of plain waterjet process. The model had successfully predicted the R_a of the cleaned automotive parts within the limit of this study. A confirmation test at optimum parameters was later conducted to verify the improvement of quality characteristic during the waterjet paint removal process. The recommended optimal parametric combinations for better R_a were found to be waterjet pressure of 34 MPa, traverse rate of 500 mm/min, standoff distance of 10 mm, number of passes of 1 and lateral feed of 0.6 mm. It can be concluded that the selected optimal combination of plain waterjet parameters satisfies the actual requirement for cleaning of automotive paint in real practice. The results from the present work based on RSM and qualitative modelling are valuable in analysing the effect of various waterjet processing parameters thus attaining an appropriate control over the cleaning efficiency of automotive paint

ABSTRAK

Keperluan pembersihan cat automotif tanpa pencemaran sekunder kini telah menjadi sesuatu yang penting secara global pada zaman kini. Teknologi jet air tekanan tinggi telah merangkumi aplikasi termasuk di dalam tujuan penambahbaikan permukaan,pemesinan, pembersihan dan pemotongan bahan. Teknologi jet air tekanan tinggi dengan hanya menggunakan air selalunya digunakan untuk tujuan pembersihan kerana ia adalah konsep mesra alam semulajadi yg berteraskan hampir sifar pencemaran ke persekitaran. Kertas kerja ini dijalankan bertujuan untuk mengkaji kesan parameter operasi teknologi jet air tekanan tinggi kepada kualiti permukaan semasa pembersihan cat automotif menggunakan kaedah response surface methodology (RSM). Kesan kekasaran permukaan dan topografi telah dianalisis. RSM, analysis of variance (ANOVA), factorial separa dengan dua tahap dan central composite design (CCD) telah digunakan untuk mengoptimumkan parameter jet air bertekanan tinggi bagi mencapai penyingkiran cat yang berkesan. Kajian mendapati suapan sisian dan tekanan jet adalah faktor pengawal paling penting dalam menentukan kriteria prestasi pembersihan. Model matematik telah dibentuk menggunakan linear regression analysis untuk menjangka kekasaran permukaan dari segi parameter pembersihan menggunakan proses jet air bertekanan tinggi. Model itu telah berjaya mengenalpasti kekasaran permukaan bahagian automotif yg telah dibersih dalam limit kajian ini. Untuk mencapai penyingkiran cat automotif yg berkesan, kenalpasti kepada pembaikan dalam kriteria kualiti telah dibuat menggunakan ujian pengesahan bersandarkan aturan mula parameter yang telah dipilih. Gabungan parameter optimum yg disarankanadalah 33.6 MPa untuk tekanan jet, 500 mm/min untuk kadar lintasan, 10 mm untuk jarak antara nozel dan permukaan, 1 lintasan cucian dan 0.7 mm untuk suapan sisian. Disahkan bahawa gabungan parameter optimum jet air bertekanan tinggi yg dijumpai adalah pada kadar memuaskan untuk keperluan sebenar dalam penyingkiran cat automotif. Ia adalah sesuatu yang jelas bahawa lambakan kajian menggunakan RSM, model kualitative dan dapatan daripada eksperimen sepertimana dijumpai dalam kajian ini akan menjadi sesuatu yang bermakna dalam meneliti kesan kebanyakan proses parameter jet air untuk mendapatkan kawalan yang sesuai keatas pembersihan yang berkesan dalam amalan yang sebenar.

TABLE OF CONTENT

LIST OF TABLES

LIST OF FIGURES

UMP

LIST OF SYMBOLS

$\sigma_{0.2}$	Yieldstrength
σ_b	Ultimate strength
E	Elastic modulus
p	Pressure
n	Number of passes
u	Traverse rate
s	Standoff distance
f	Lateral feed
R_a	Surface Roughness
V	Material removal rate
R_w	Surface waviness or striation
h	Depth of cut
w	Kerf width and taper
d_j	Waterjet diameter
α	Impact angle
l_n	Nozzle length
D	Nozzle diameter
d_p	Abrasive particle diameter
m_a	Abrasive mass flow rate
H_p	Abrasive particle hardness
$f(d_p)$	Abrasive particle size distribution
H_d	Hardness
σ_f	Flow strength
GPa	Gigapascal
MPa	Megapascal
psi	Pound per square inch
mm	Millimeter
µm	Micrometer
min	Minute
%	Percentage
α	Significant level

LIST OF ABBREVIATIONS

RSM	Response Surface Methodology
CCD	Central Composite Design
CNC	Computer Numerical Control
DOE	Design of Experiments
R-Sq	Coefficient of determination
R-Sq(pred)	Predicted R Square
R-Sq (adj)	Adjusted R Square
StdOrder	Standard order

CHAPTER 1

INTRODUCTION

1.1 Introduction

A removal process of paint in automotive coating is frequently used in vehicle component recycling industry (Zhang & Chen, 2015). The necessity of utilizing and recycling automotive components without generating secondary pollution from paint removal procedure has become recent main concern globally. Waterjet cleaning is a new method for paint removal and is getting wider recognition due to its environmental friendly feature compared to mechanical cleaning processes such as sand blasting, brushing with water, hydropneumatic cleaning, controlled dry sanding, low pressure water projection and low pressure water spray (Folkes, 2009).

Automotive is a fast-growing sector with huge quantity of products are manufactured and painted annually. Increasing stringent checks of substrate and coating thickness as well as paint tolerances are most common problems occured in the automotive sector. To lessen dumping expenses, product processing and reproduction, various companies discover alternative recycling methods by reusing rejected products. Automotive parts such as rims, bumpers, bodies, boot lids, doors, couplings and engine parts could be stripped off and cleaned for recycling purposes as they have large surface area.

Paint is a combination of binders, additives, pigments, and solvents that can be manipulated for both good and bad purposes (Sanmartín, Cappitelli, & Mitchell, 2014). For good purposes, paint can be used a protective coating to any surface. Common problem faced by most industries is corrosion of metal structures outdoors. These structures range from bridges to window frames and vehicles. Paint application is the most common used technique to protect automotive components. On the other hand, paint can also be manipulated for inappropriate purpose such as used painting the wall as

graffiti. In fact, graffiti does not only damage properties but also causing valuable properties to lose their values.

Before fresh coat paint is applied or rejected automotive parts are used, old paint needs to be removed first. In most automotive companies, there are three ways of removing paint from substrate surfaces which are sanding, chemical stripping and blasting. Although these methods are common practice in the industry, they have major disadvantages such as intense labour and high energy expenses, damage and degradation of parts as well as lavish waste dumping. Traditionally, chemical method is used to corrode the paint. Major disadvantages of chemical corroding include harming operator's health, the environment, and substrate surface (Carvalhão & Dionísio, 2015). Blasting can deform the product if the material is extremely thin (Pozo-Antonio, Rivas, Fiorucci, López, & Ramil, 2016). These variables are always taken into account when products are to be treated. This slightly roughens the product surface. The degree of roughening depends on the blasting method and pressure used.

Cleaner method based on physical de-coating is commercially available or is being developed to substitute solvent strippers and mechanical methods. The variances in physical properties between the coating and substrate are the main factors in this technology to terminate the bonding and remove coating from the substrate.

Currently, the needs to fulfil the requirements of production and maintenance have made the use of high-pressure waterjet technique is widely accepted in practice. This technique can be utilized in cleaning, surface treatment, machining and cutting of materials. Moreover, the waterjet process extends its usage for machining thin, hard and complex shape material. It is noted that technical surface treatment is an area of numerous scientific research interests nowadays. To achieve the purpose, many researchers employed plain waterjet. However, intense high pressure is needed to employ this method and it is limited in eradicating weak bond surfaces of the substrate. Recently, the waterjet is introduced to stone surface treatment (Aydin, Karakurt, & Aydiner, 2011). The process increases surface roughness and improved anti-slip properties; while, conserving the stone's aesthetic appearance without thermal shock, mechanical stress and production of fumes and dust. The advantages of using water medium in waterjet technology include readily obtainable, reasonably low-cost, and induces no harm to surroundings (Folkes, 2009). During waterjet cutting, dust, poisonous gases, gaseous impurities, or hazardous

materials are produced; however, it is easy to monitor. It is vital to state that waterjet method conveniently is the most efficient technology.

Despite the aforementioned advantages, waterjet technology has not found sufficient information in some of the parameter areas. Lack of information pertaining to the correlation between process conditions and paint removal impedes the improvement of waterjet technology. If the jet impinges on the momentum below critical value, paint erosion turns out to be impossible. On the other hand, if the momentum of impinged jet surpasses upper critical level, the substrate will be damaged. A complete paint removal without damaging automotive surface is seen impossible because the paint surface is incredibly thin and near to the contradiction of waterjet paint removal process. To solve the contradiction, more researches should be conducted to attain the best working condition for automotive paint cleaning. It is then necessary to understand the correlation between paint cleaning and jet properties to improve process effectiveness.

1.2 Problem statement

High cleaning efficiency and paint erosion with minimum substrate damage is the main objective in paint removal process. This objective is commonly became the major problem to achieve in cleaning of paint. Most of current related researches in cleaning process emphasize laser cleaning method. Laser cleaning overall cost including device and labour is pricey. In addition, cleaning by laser can cause damage to substrate and alteration of substrate colour. Laser cleaning application is limited to historical and ornamental usage due to its cost which is nearly 20 times more expensive than conventional method (Sanmartín et al., 2014). Several number of researches on stone emission using laser ablation technology demonstrated that laser cleaning produced environmental health hazard and failed to follow security and health requirements despite of its rapid development (Vergès-Belmin et al., 2003). Low environmental health hazard is produced by waterjet cleaning compared to laser cleaning because waterjet technology uses water as medium to remove paint in the cleaning operation.

Since researches on paint cleaning focus more on laser ablation, this leads to scarce of interest in investigating waterjet cleaning application. It was observed that researches on waterjet cleaning are limited particularly concentrating on parameters such as standoff distance, waterjet pressure, kinetic energy, traverse rate and attack angle. It was further discovered that none of these works were conducted with more than single

pass cleaning. Recent studies on multiple cleaning pass concluded that in stone cleaning, two-pass cleaning with laser ablation show high efficiency and low damage compared to single pass cleaning. This result was achieved because laser cleaning was performed by lowering irradiance level (lower than damage threshold) compared to single cleaning pass (Penide et al., 2013). Therefore, it is interesting to study the effect of multiple passes parameter in waterjet paint cleaning as similarly conducted in laser cleaning process. Furthermore, paint removal process using waterjet is still new with very few studies were conducted to analyse parameters optimization and surface integrity. Thus, it is vital to study the effect of multiple passes with pure waterjet paint cleaning to improve the process; while, minimizing substrate damage by using optimization technique.

The present study concentrates on the analysis of multiple passes effects in pure waterjet paint cleaning. New multiple passes treatment technique in pure waterjet cleaning was employed to examine its effect on surface roughness. In addition, visual inspection technique was also applied to check the surface physical. Apart from that, response surface methodology (RSM) involving two level factorial designs were used for process parameters optimization. Significance of the model was evaluated by ANOVA analysis and regression equations were established.

1.3 Objectives

The objectives of the present research are as follow:

i. To investigate the effects of multiple passes treatment in waterjet cleaning on paint removal of automotive parts in term of surface quality.
ii. To evaluate the significance of each waterjet parameter using RSM for effective paint removal process.
iii. To determine optimum combination of waterjet parameters using RSM for automotive paint removal process.

1.4 Organization of thesis

This thesis mainly contains of five chapters which are the combinations of an introduction, literature review, research methodology, result and discussion as well as conclusion. Chapter one explains in detail about title of the thesis, scope of the thesis,

problem statements and objectives of the thesis. Chapter two reviews previous studies related to this study. These literatures help in having better understanding about waterjet cleaning and paint removal. Meanwhile, Chapter three discusses the experiments and analysis procedures employed in the study and the scopes of present study. Chapter four explains the results from the experiments and result discussion at length. Finally, Chapter five discusses the conclusions drawn from the results. Additionally, recommendations on future works are also presented in this chapter.

UMP

CHAPTER 2

LITERATURE REVIEW

2.1 Introduction

The purpose of this chapter is to review on the studies done by other researchers in the past related to this study. These literatures cover the research done on paint removal method, waterjet paint cleaning method and optimization of waterjet machining process using RSM.

2.2 Paint

Paint is generally prepared by combining various pigments (such as iron oxide, carbon black or aluminium among others) with mineral solvent and synthetic resins/ binder (thermoplastics or thermostable); which allow the substrates and paint to be bonded together (Sanmartín et al., 2014). Pigments can be categorised into organic and non-organic substances. It provides colour for the paint and conserves any surface from corrosion, erosion and wears off. Synthetic resin or binder which is a polymeric substance protects the paint and holds the substances together. The solvent component in paint is used to allow paint to spread and flow easily. Additives such as plastifying are mixed to enhance adherence, fluidity, plasticity and thickness properties.

Automotive paint typically consists of similar conventional paint composition; but it normally needs combination of multilayer coatings. A single coating on automotive component is not recommended; since it is lack of environmental resistance, anticorrosion and adhesion incapability. Generally, two common types of automotive paint finishing such as solid and metallic colour are used. The difference between these two types is that metallic colour has additional layer known as metallic basecoat. The

composition and thickness of metallic automotive coating are electro coat, primer coat, metallic base coat and top clear coat as illustrated in Figure 2-1. Most coating layers have chemical composition of C, O, Al, Si, Ti and other additional elements.

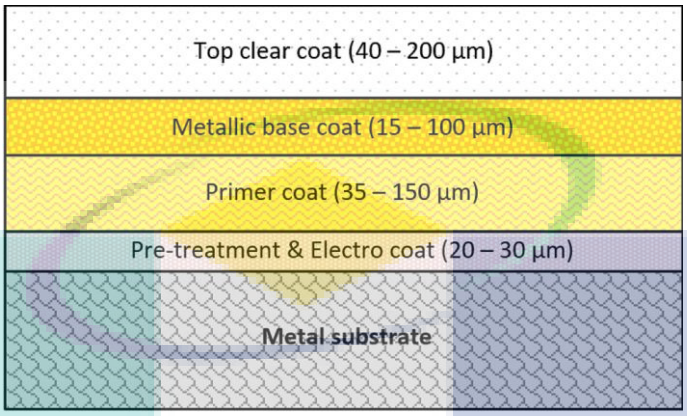

Figure 2-1 Cross-sectional of metallic colour for automotive paint and its approximate layer thickness for each coating

Source: (Khairul, Abdul, Noor, & Suhaimi, 2018).

Each automotive paint layer is applied and has its unique function. This particular automotive coating sorted in specific order has dissimilar function and material as shown in Figure 2-2.(Akafuah, Poozesh, Salaimeh, Patrick, & Lawler, 2016)

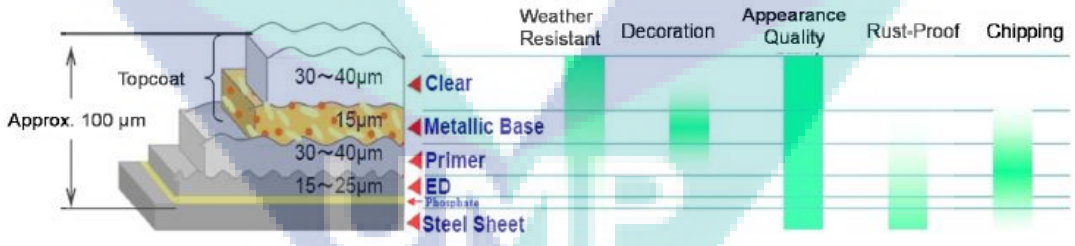

Figure 2-2 Automotive paint, their thickness layer and respective function.

Source: (Akafuah et al., 2016).

2.3 Paint removal method

Removal or de-coating process of cleaning the contaminants, coating materials and deposits from the substrates of manufacturing tools parts are described as important in automotive industrial area. Application of the process can be found in numerous areas including paint erosion process. In general, the techniques used for effective paint

removal can be classified into chemical and mechanical cleaning, laser ablation and waterjet cleaning as illustrated in Figure 2.3.

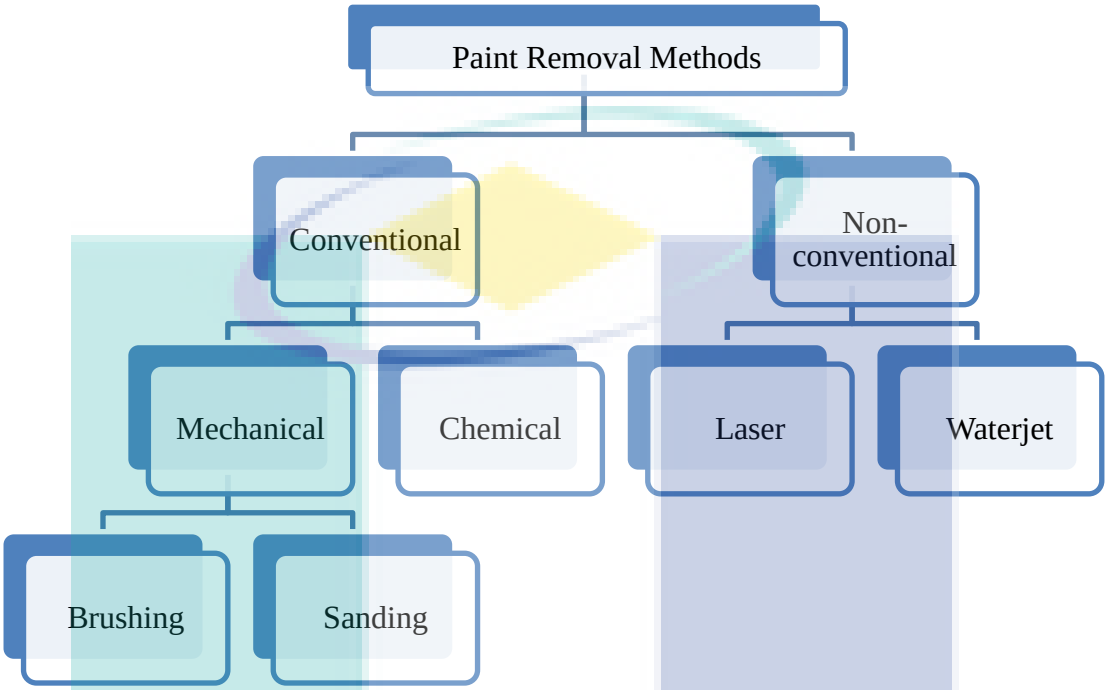

Figure 2-3 Classification of paint removal methods

Conventional procedures for cleaning paint include mechanical methods (e.g. low pressure water spray, hydropneumatics cleaning, low pressure water projection, water brushing and controlled dry sanding) and chemical product application method (e.g. acids) (Carvalhão & Dionísio, 2015). Summary of previous studies on paint removal techniques is presented in Table 2-1.

Table 2-1 Summary of previous studies on different paint removal methods

NO	Article	Machining Method	Paint	Substrate
1	(Carvalhão & Dionísio, 2015)	mechanical soft-abrasive cleaning, chemical cleaning	alkyd-paint sprays	Calcareous stones, marble, limestone
2	(Gomes, Dionísio, & Pozo-Antonio, 2017)	Anti graffiti coating, Chemical cleaning, Laser cleaning, Waterjet		Various materials
3	(Pozo-Antonio, Rivas, Fiorucci,	Chemical cleaning, mechanical cleaning and laser ablation	spray	Granite

	L??pez, & Ramil, 2016)			
4	(Sanmartín et al., 2014)	Chemical cleaning, Physical cleaning, Biological cleaning	spray	Various materials
5	(Moura, Flores-Colen, de Brito, & Dionisio, 2017)	Anti graffiti product, high-pressure water washing, chemical graffiti removers	Spray, marking pen	Mortar
6	(Chapman, 2000)	Laser cleaning, Low pressure steam cleaning	Spray, emulsion paint, gloss paint	Stones
7	(Samolik et al., 2015)	Laser ablation, Chemical cleaning, Mechanical cleaning	aerosol paints	limestone, sandstone, plaster, and brick
8	(Weaver, 1832)	Laser cleaning, Chemical cleaning, Mechanical cleaning	Various type	Various materials
9	(Mazzinghi & Margheri, 2003b)	Laser cleaning	synthetic paint	Marble
10	(Penide et al., 2013)	Laser cleaning	spray	Igneous rock
11	(Ortiz et al., 2013)	near-infrared (IR) and ultraviolet (UV) laser pulses cleaning	spray	dolomitic white marble
12	(Rivas, Pozo, Fiorucci, Lopez, & Ramil, 2012)	Laser cleaning	spray	Granite
13	(Matsui et al., 2006)	Laser irradiation cleaning	Marking pen	Mortar
14	(Fiorucci, López, Ramil, Pozo, & Rivas, 2013)	Laser cleaning	spray	Granite
15	(Sanjeevan, Klemm, & Klemm, 2007)	Laser cleaning	spray	Mortar
16	(Andriani, Catalano, Daurelio, & Albanese, 2007)	Laser cleaning	Marker and pen	Calcareous stone
17	(Costela, García-Moreno, Gómez, Caballero, & Sastre, 2003)	Laser radiation	spray	Glass, steel, wood, marble and concrete
18	(Ramil, Pozo-Antonio, Fiorucci, López, & Rivas, 2017)	Laser cleaning	spray	Granite

19	(Careddu & Akkoyun, 2016)	plain high-pressure water-jet	spray	Carrara marble

2.4 Conventional method

2.4.1 Chemical method

Generally, painted surface is soaked in special chemical solution for chemical cleaning application; as a result, the paint eventually erodes. These chemical products (which typically contain chloride, phenol, methyl ethyl ketone, and methylene) result in permanent damage to the substrate because they are able to penetrate deeper into it. This is common as chemicals are extremely destructive and contain substances that are poisonous; thus, creating severe health and environmental threats (Sanmartín et al., 2014). Although chemical cleaning is commonly applied in paint removal process, the liquid waste produced is extremely damaging to the environment and the process capacity is low (Zhang & Chen, 2015).

2.4.2 Mechanical method

On the other hand, mechanical paint cleaning is a process, whereby, paint is eradicated using mechanical friction between a friction medium and painted surface. Mechanical methods can cause damage to the texture and unexpected material elimination on the surface. Contaminants with huge size of especially fine dust particles into air was produced by using these techniques (Sanmartín et al., 2014). Moreover, this technique is incompatible for large scale production and inefficient (Zhang & Chen, 2015). A recent study was conducted to compare mechanical and laser cleaning of graffiti spray on artificially aged stone by SO_2 exposure method. Mechanical method with different micro abrasives (Hydrogommage$^{@}$ – combining action of water, air and micro abrasive-silica or aluminium silicate and IBIX$^{@}$ – combining action of micro abrasive-silica or calcium carbonate and air), and a ns Nd:YVO4 laser. The authors agreed that SO_2 exposure influences mechanical and laser cleaning techniques. Greater global colour changes and high difficulty of cleaning for aged samples were observed. They found the procedure that achieved the best result is Hydrogommage$^{@}$ with silica abrasive due to a combination of low morphological harms and acceptable paint erosion applied to the stone (Gomes, Dionísio, Pozo-antonio, Rivas, & Ramil, 2018). In soft- abrasive blasting,

it is compulsory for cleaning site to be enclosed and the operator to be protected from fine dust particle, eye injury and loud noise (Carvalhão & Dionísio, 2015).

2.5 Non- conventional method

2.5.1 Laser method

Laser cleaning or laser ablation method utilizes the benefit of fibre optic propagation in removing the paint on monuments surfaces (Costela et al., 2003; Fiorucci, Lopez, Ramil, Pozo, & Rivas, 2013; Mazzinghi & Margheri, 2003a). The attempt of removing sprayed paint on construction material (glass, steel, wood, marble and concrete) by laser with third and second harmonic results in identical cleaning efficiency (Costela et al., 2003). Whilst, paint thickness sprayed on mortar can be reduced by pulsating laser irradiation at the effective zone; it is constant at the ineffective zone eventhough laser actually influences changes (Sanjeevan et al., 2007). Barletta et al. (2006) conducted paint stripping process using high power diode laser from aluminium sheets coated with single layer epoxy polyester paint. The researchers studied the influence of main variables such as interaction time, power density, absorption coefficient number of passes and length of paint removal efficiency using full factorial experiment design. They discovered the effectiveness of paint removal is indicated by the depth of paint deletion. In fact, identification of the best solution to lead paint removal process is also obtained (Barletta, Gisario, & Tagliaferri, 2006).

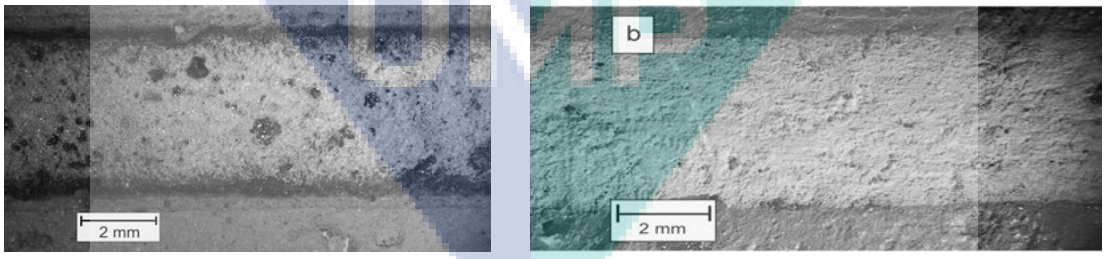

(a) (b)

Figure 2-4 Optical Microscope image cleaning of Pink Morelia Quarry stone using high power diode laser at operating condition of 800 W/cm^{2,} sample speed 10 mm/s with (a) single laser pass (b) two laser pass.

Source: (Penide et al., 2013).

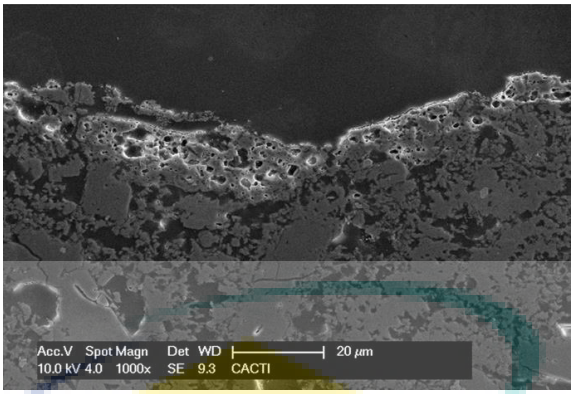

Figure 2-5 Image cleaning of Pink Morelia Quarry stone using high power diode laser at operating condition of 90 W, 800 W/cm^2, 350 J/cm^2, 2 laser passes, sample speed 10 mm/s as observed by electronic microscope on the heat affected zone cross-section.

Source: (Penide et al., 2013).

Penide et al. (2013) studied paint removal of quarry stone using high power diode laser. They found that the optimum parameter of stone removal paint is by using two laser passes. The comparison between single and two laser passes is shown in Figure 2-4; whereby two laser passes show lower density of black spots. This black spot corresponds with the grains; an area of the stone that was melted. This melted stone is caused by laser beam during paint removal process. Another research demonstrated that two cleaning passes create smaller heat affected zone (HAZ) than single cleaning pass which is proven by the absence of stone cracking on the treated zone (Penide et al., 2013)

In removing marking pens on mortar, it was found that substrate damage can be eradicated by laser irradiation via repetitive low energies at various levels (Matsui et al., 2006). Comparison between conventional methods and pulsating laser cleaning to clean paint on white marble shows that better cleaning performance is attained using laser cleaning as shown in Figure 2-6. Despite the lavish cost of extensive application due to its high processing time, they found that pulsed laser cleaning technique is suitable for rapid cleaning of inaccessible or minor surfaces (Ortiz et al., 2013).

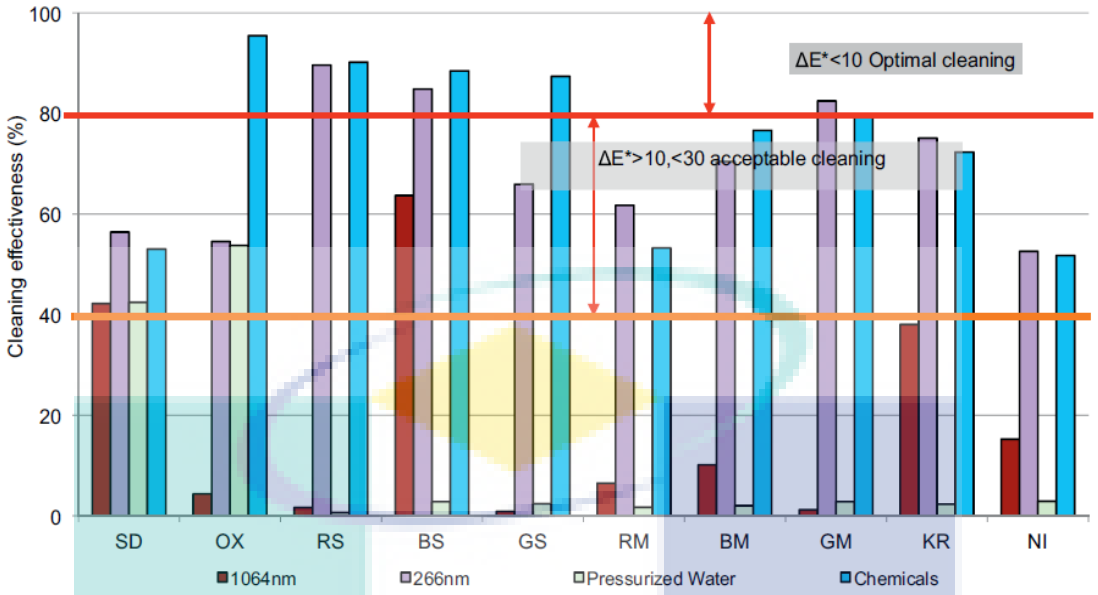

Figure 2-6 Cleaning effectiveness of laser at near-infrared (IR) and ultraviolet (UV) laser pulses in comparison of pressurized water and chemical methods

Source: (Ortiz et al., 2013).

Higher ablation rate without any thermal damage is attained by altering Nd :YAG laser working in free running (FR) regime, with duration pulse of 20 ms which is faster than conventional system (>200 ms) (Mazzinghi & Margheri, 2003a). In other method, shifting number of cleaning passes shows that two cleaning passes by using laser cleaning is optimal to eradicate paint from quarry stone surface using high power diode laser method (Penide et al., 2013). In an experimental laser ablation tests on 4l new pens and markers (categories include water-based, fluorescent, metallic paint, waterproof inks, permanent, acrylic tempera), paints on the stones show satisfactory cleaning efficiency without substrate damage (Andriani et al., 2007). Different characteristics of silicate minerals in granite (biotite, plagioclase, quartz and K-feldspar) impede laser cleaning which leads to watchful removal paint on this substrate (Ramil et al., 2017). Researches on the effect of removing paint on granitic stones using Nd:YVO4 laser show different results for different colours with silver paint remains in the substrate due to its chemical composition (Rivas et al., 2012). Among the disadvantages of laser cleaning include lavish cost, substrate colour alteration and substrate damage. It was found that laser ablation application is constrained by its ornamental and historical usages as conventional method is almost 20 times cheaper (Sanmartín et al., 2014). Cleaning period of laser cleaning using Nd:YAG laser at 1064 nm also consumes time as it normally takes several

weeks to remove paint on the stone surfaces as found in Avebury Stone Circle (Wiltshire, UK) (Chapman, 2000). Lack of research on laser cleaning method on stone emission proves that rapid development of this method is unsuccessful to satisfy the health and security assessment while creating environmental health threat (Vergès-Belmin et al., 2003). In a comparative study on cleaning method using chemical, physical and laser cleanings, the results demonstrate satisfactory evaluation on paint cleaning and the cleanings are harmful on granites (Pozo-Antonio et al., 2016).

2.5.2 Waterjet cleaning Method

The use of waterjet technology has been extended in various applications involving material cutting, deburring and surface cleaning (Chizari, Barrett, & Al-Hassani, 2009). The main objective of waterjet cleaning is to complete the coating or paint removal without any erosion or damage to substrate surface. Among the advantages of this method are anti-heat generation and thermal degradation of work material, minor maintenance, clean and sharp cut, no tool wear and powder less environment (Balasubramaniam et al., 1963). Other advantages include the none removal of substrate, no surface deformation, no abrasive if pure water is used and better cleaning rates compared to chemical technique (Folkes, 2009a). From technical-economic perspective, a research on marble cleanse using waterjet cleaning showed when optimum waterjet working parameters combination is selected in the case of rustic or saw plane (i.e. bush-hammered) stone surfaces, the process succeeds in removing paint (Careddu & Akkoyun, 2016). In general, paint removal using waterjet basically involves erosion process caused by targeted discrete droplets on the work piece surface at high pressure and speed jet of water stream. Extreme high pressure is projected as a result of water kinetic energy transformation whereby most materials from impacted areas are removed by emission of stress waves on the target surfaces. The performance of waterjet cleaning is estimated and determined by its process parameter settings including standoff distance (s), traverse speed or feed rate (u) and waterjet pressure (p). The magnitudes of these process parameters are significant and will define the process output features for waterjet application.

2.6 Waterjet technology

The categories of waterjet machining parameters are classified into two types which are output and input parameters. These working parameters include: (M. and Kovacevic, 1998)

A) Output parameters:
   a. Geometrical and dimensional accuracy
   b. Material removal rate (V)
   c. Kerf characteristics: Surface waviness or striation (R_w), Burr formation, Surface roughness (R_a), Depth of cut (h), Kerf width and taper (w),

B) Input parameters:
   a. Hydraulic parameters: Waterjet diameter (dj), Water pressure (p)
   b. Cutting parameters: Number of passes (n), Nozzle traverse speed (u), Impact angle (α), Standoff distance (s)
   c. Mixing and acceleration parameters: Nozzle length (l_n), Nozzle diameter (D)
   d. Abrasive parameters: Abrasive particle diameter (d_p), Abrasive mass flow rate (m_a), Abrasive particle hardness (H_p), Abrasive particle shape, Abrasive particle size distribution ($f(d_p)$)
   e. Target material parameters: Hardness (H_d), Elastics Modulus (E), Flow strength (σ_f),

2.7 Influence of waterjet machining parameters on surface topography

One of the main parameters in waterjet technology is waterjet pressure. Pressure level significantly determines the amount of kinetic energy produced by waterjet machine. Waterjet pressure is also related to material removal rate and depth of penetration. Another main parameter in waterjet machining is traverse rate which determines the quality of surface removed. The most significant parameter that relates with traverse rate is exposure time. High exposure time or low traverse rate allows water particle to erode more surface layers. Standoff distance is also important in determining surface removal by waterjet machining. The distance between workpiece and nozzle is called standoff distance. The magnitude of standoff distance is important in determining

the shape of kerf profile. Other waterjet parameters are abrasive type, lateral feed and number of cleaning passes.

Surface roughness of aluminium alloy 5005 increases as waterjet pressure enhances. Increasing pressure elevates water kinetic energy to remove more materials; thus, resulting in high surface roughness as presented in Figure 2-7 (b). A lower federate allows the overlapping of machining action and additional waterjet molecule to hit the target material. This is due to low traverse rate causing high exposure time to the jet for surface removal which increases surface roughness as presented in Figure 2-7 (c). High standoff distance results in high surface roughness as presented in Figure 2-7 (d). This is due to the reflection of water droplet disturbing the incoming waterjet at low standoff distance while its effect reduces at high standoff distance. Surface roughness increment is a result of the increased number of passes as presented in Figure 2-7 (a). It is noted that high surface roughness is attained since additional number of passes makes the surface rougher due to bombardment of particles on the same surface. (Azhari, Schindler, & Li, 2013).

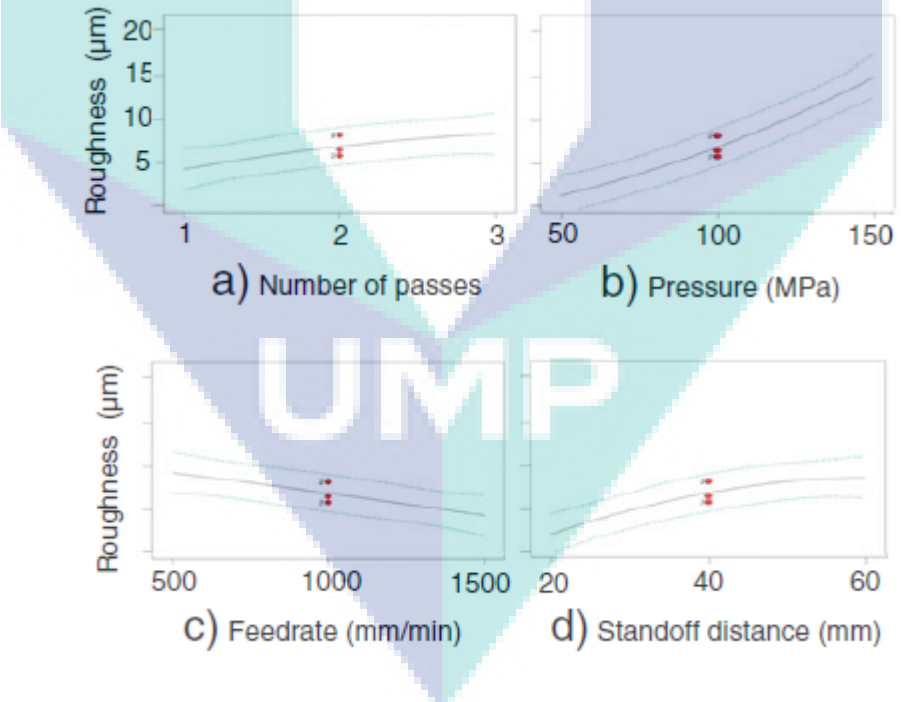

Figure 2-7 Effect of waterjet on the, a) number of passes, b) pressure, c) feed rate and d) standoff distance on surface roughness.

Source: (Azhari et al., 2013).

In another investigation on machining cast iron using abrasive waterjet, it was found that surface roughness decreases as waterjet pressure elevated as shown in Figure 2-8 (a). Smoother surface is obtained as abrasive particles break into smaller size. Surface roughness increases as traverse rate gets higher as exhibited in Figure 2-8 (b). The reason for this is less particles pass through a unit area with high traverse rate. As a result, there is less number of impacts and surface becomes rougher. It is also noted that the higher standoff distance, the higher surface roughness is as shown in Figure 2-8 (c). There is high possibility that exposure of the jet to external drag from the surroundings causes waterjet to spread at higher standoff distance. This reduces jet kinetic energy and causes enlarged waterjet diameter. The end result shows that surface roughness is smoother at the top of the surface and higher at the bottom of the machined surface. (Selvan & Raju, 2012)

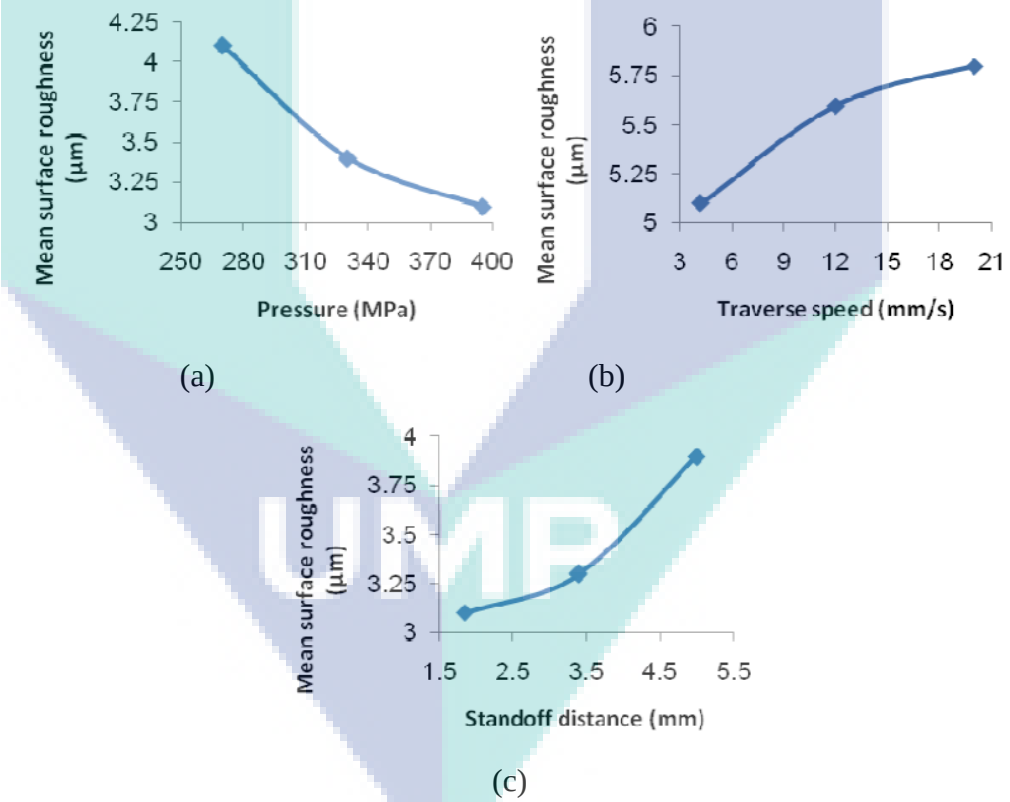

Figure 2-8 Effect of, a) waterjet pressure, b) traverse rate and c)standoff distance on surface roughness.

Source: (Selvan & Raju, 2012).

Rougher cut surface can be obtained if waterjet pressure is increased in cutting stainless steel as shown in Figure 2-9 (a). High waterjet pressure enhances the possibility

of collision between particles. High tendency of collision occurs because of the acceleration and additional energy disbursement from abrasives by waterjet. A similar result as Selvan et al. was found by Badgujar and Rathi in cutting stainless steel by waterjet as shown in Figure 2-9 (b); whereby at higher level of traverse rate, surface roughness is higher (Badgujar & Rathi, 2014) .

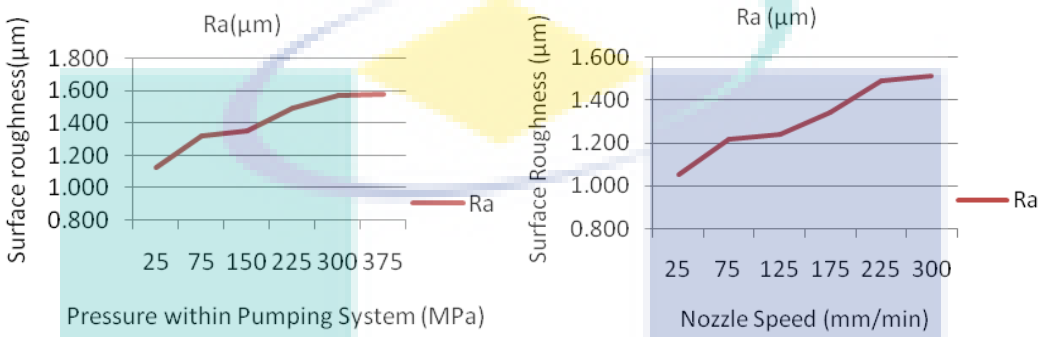

(a) (b)

Figure 2-9 Effect of, a) waterjet pressure and b) traverse rate on surface roughness

Source: (Badgujar & Rathi, 2014).

Studies on surface roughness of three granites (Rosa Minho, Giresun Vizon and Balaban Green) machined by varying abrasive waterjet parameter was conducted previously. It was found that surface roughness is the highest for medium-grained granite and the lowest for fine-grained granite. The varying abrasive waterjet parameters in response to mean surface roughness are presented in Figure 2-10. For all rocks, traverse rate shows high value at increased surface roughness as presented in Figure 2-10 (c). In the case of waterjet pressure, it is observed that surface roughness of all rocks also portrays high value at high waterjet pressure as shown in Figure 2-10 (b). This is because of the increased water kinetic energy and disbursement of energy from abrasive to the affected area that is bombarded by water particles. In Figure 2-10 (c), all granites show high surface roughness at increased standoff distance. The effective jet diameter is inversely proportional to the standoff distance which reduces as the standoff distance increases (Aydin et al., 2011).

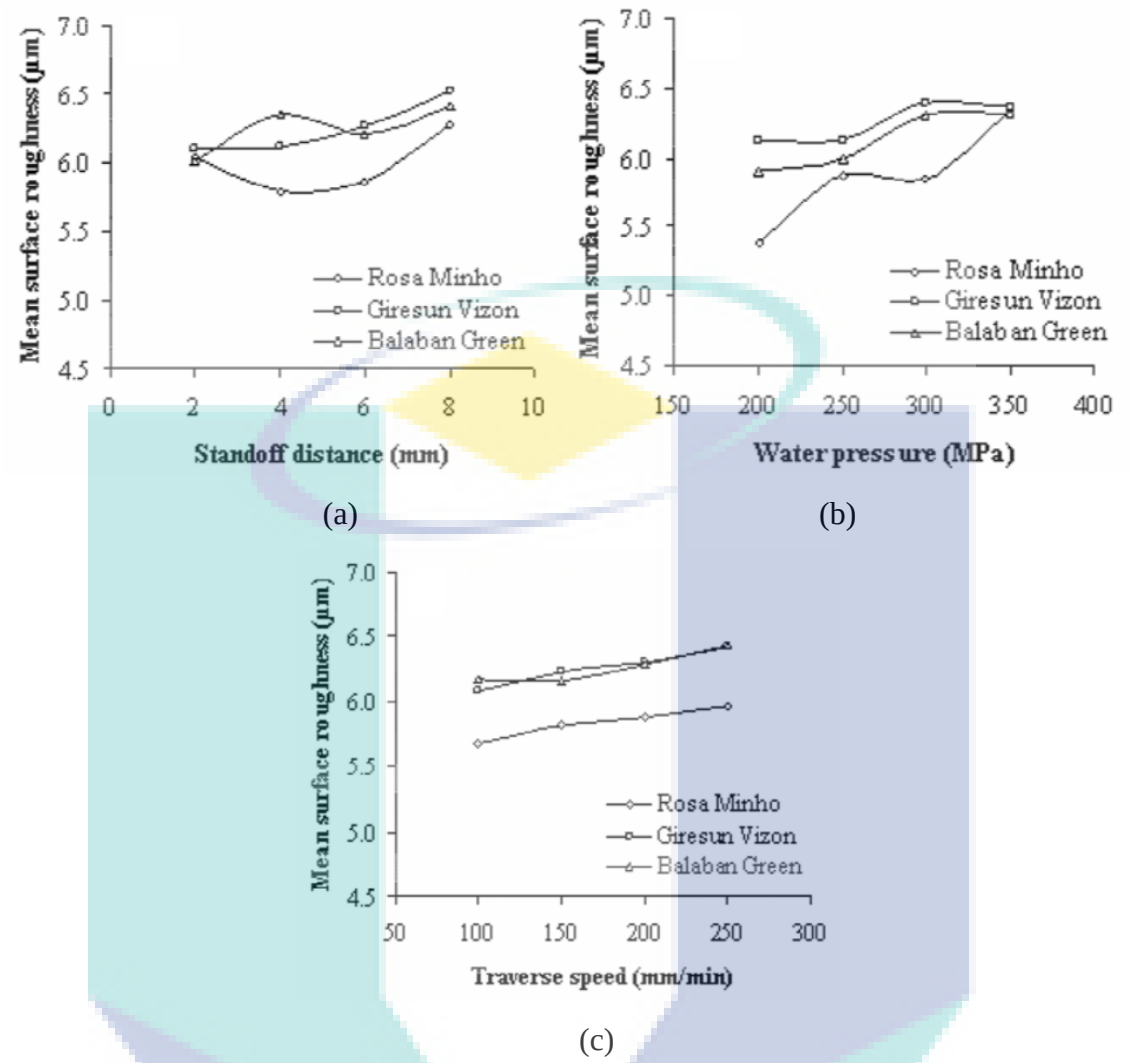

Figure 2-10 Effect of, a) waterjet pressure, b) standoff distance and c) traverse rate on surface roughness

Source: (Aydin et al., 2011).

Surface roughness test is the main parameter that describes surface quality of a substrate. In determining surface quality of abrasive waterjet machining, average roughness (*Ra*) measurements have become the standard default representation for machined surface finish. In measuring *Ra* surface finish, minor length inspection to represent the entire area is conducted since basic assumption of average roughness (*Ra*) measurements is the surface finish is uniformed across the whole surface. A study to establish damage thresholds was performed based on the variations of root mean square roughness (RMS) induced on surfaces after cleaning process based on standard deviation of RMS values measured in reference surfaces before cleaning process (Carvalhão & Dionísio, 2015).

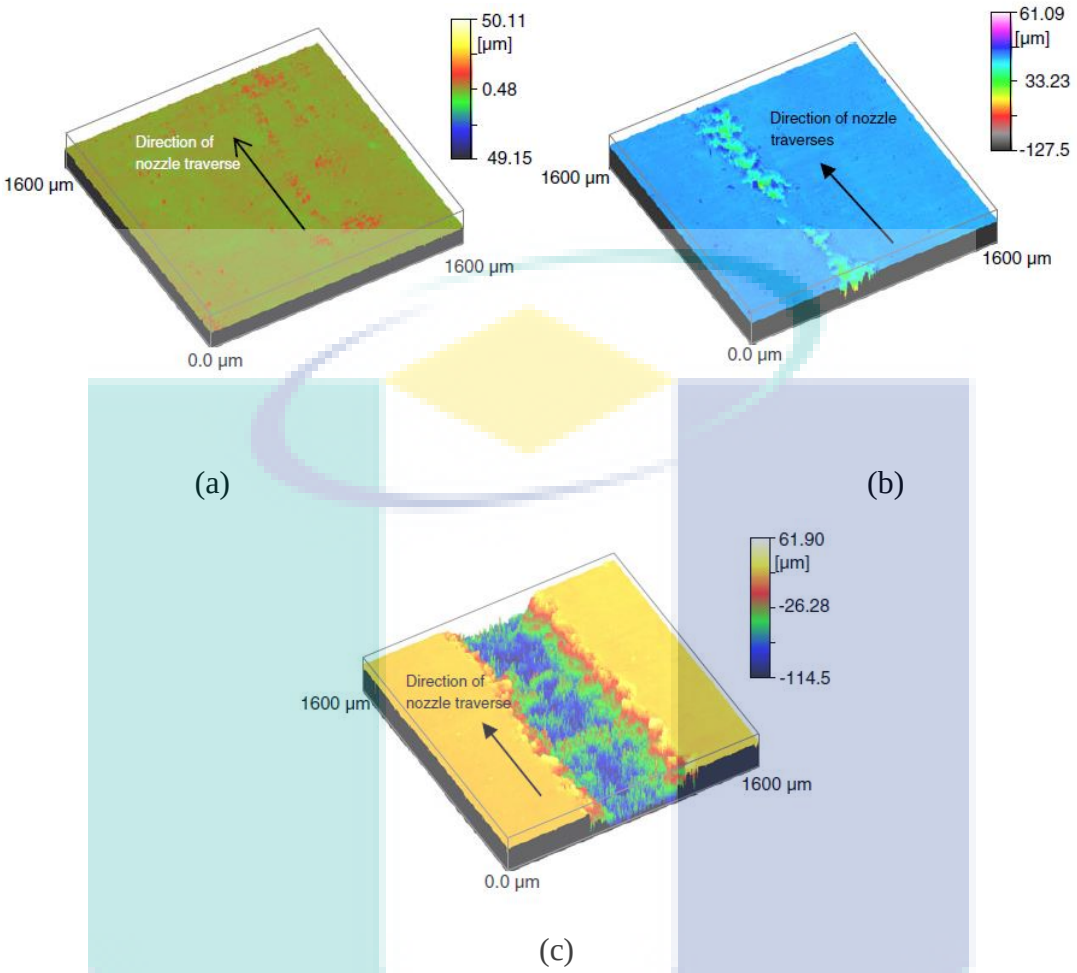

Figure 2-11 3D images of surface structure for all groups by n = 2, p = 100 MPa, u = 1500 mm/min, s = 20 mm, R_a = 0.54 µm, (a) by n = 2, p = 100 MPa, u = 1500 mm/min, s = 20 mm, R_a = 0.54 µm (b) by n = 1, p = 100 MPa, u = 500 mm/min, s = 40 mm, R_a = 6.78 µm and (c) by n = 2, p = 150 MPa, u = 1500 mm/min, s = 40 mm, R_a = 0.56 µm

Source: (Azhari et al., 2013).

The differences between average peak to valley height (R_z) and average roughness (R_a) in the measurement of surface finish of abrasive waterjet cut surfaces were studied and analysed. Pocket Surf® PS1 profilometer was used to measure surface finish. There is an argument that surface waviness must be involved in the measurement of overall surface roughness since there is the existence of some level of striations in abrasive waterjet machined surfaces. The recommendation was to use *Rz* as a measure of surface roughness since it captures the striations on the machined surface when measured from the lowest part of workpiece over jet exit area. They found that in abrasive waterjet cutting, *Ra* measurement is applicable since the measurement highly depends on the

abrasive size and type (Miles, 2013). Another researcher in National Institute of Standards and Technology also studied surface roughness measurement conditions and sources of uncertainty using stylus instrument. Measurement system uncertainty for R_a was analysed and deduced to be from uncertain components of deviation in calibration constants, variation in R_a values due to non-linearity in instrument transducer and uncertainty in vertical and horizontal instrument resolution (Vorburger et al., 2009). A study on peening aluminium alloy 5005 using waterjet was conducted. The study categorized surface roughness of the experiments into three groups including below 1 µm, 1-10 µm and more than 10 µm. 3D image of surface structure for the groups are displayed in Figure 2-11. In Figure 2-11 (a), surface removal is hard to be observed and nearly zero. However, in Figure 2-11 (b), the erosion is more significant with non-constant removal width and track. This moderate removal is within the range of valley-to-peak 2.8 to 4.5 µm. Meanwhile, in Figure 2-11 (c), the removal rate is observed to be severe with constant width removal and track without interruption (Azhari et al., 2013).

2.8 Optimisation of waterjet machining process using Response Surface Methodology (RSM)

Response Surface Methodology (RSM) approach is a combination of statistical analysis together with mathematical model; which is developed to obtain and optimize control parameter of machining operation. In this approach, two main response surface designs are utilized Box-Behnken designs and central composite design (CCD). The objective of the experiment and the number or sizes of factor investigated are the main determinants to choose which experimental design is suitable. In comparing two response surface design approaches, central composite design requires a lower number of runs for 2 factors; therefore, was chosen for analysing data of this experiment.

Response surface methodology approach and central composite design were successfully executed for modelling the correlation between waterjet cleaning parameters and the measurement of surface roughness. Based on the second order mathematical model from CCD, if a quality surface roughness is desired, abrasive waterjet is suitable for thin sheet stamping because of its ability to generate distortion free parts of difficult profile (R. Kovacevic, n.d.). Babu and Muthukrishnan employed RSM to obtain optimum parameter which minimizes surface roughness in machining Bras-360 using abrasive waterjet. From the analysis, they discovered that waterjet pressure is the main influence

of surface roughness value and Ra value is higher by 33%; although waterjet pressure increases by 25% (Babu, M. Naresh, 2014). Shanmugam et al. found that by using abrasive waterjet in machining 7007 Aluminium Metal Matrix Composite, RSM design of the experiment shows that taper angle and surface roughness are significantly influenced by waterjet pressure and waterjet traverse speed respectively. The optimum waterjet parameter obtained manages to achieve minimization value of taper angle and surface roughness. The regression mathematical model from RSM analysis obtained in their research concluded that the difference between predicted and experimental value is less than 5% (Shanmugam et al., 2019).

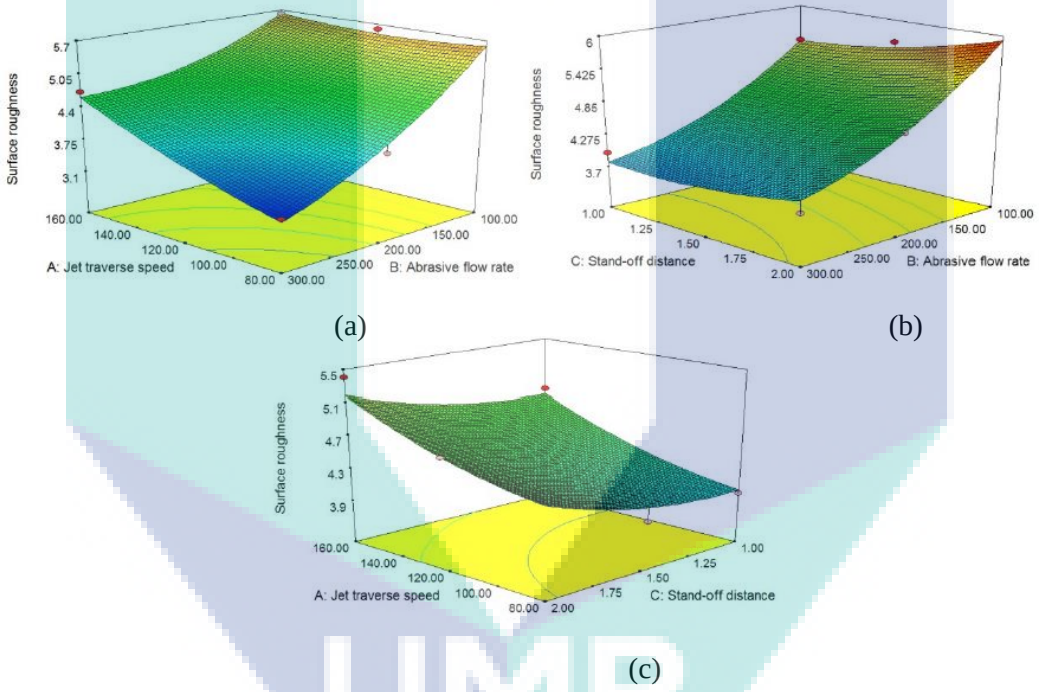

Figure 2-12 Response surface plot of surface roughness shows the function of, a) jet traverse speed and abrasive flow rate, b) stand-off-distance and abrasive flow rate and, c) jet traverse rate and stand-off-distance for cutting high speed steel by using abrasive waterjet machining.

Source: (Adalarasan Ramalingam, 2015)

Andalarasan and Santhanakumar studied the implementation of response surface methodology for machining high speed steel using abrasive waterjet. The response surface plot is illustrated in Figure 2.12. Surface finish is high at the increased jet traverse rate; while the surface is better at higher flow rate of fine abrasive. An improved surface characteristic with effective surface cut is obtained at lower standoff distance. Optimal

parameter using RSM was found as a combination of standoff distance at 1.2 mm, jet traverse rate of 80.50 mm/min and abrasive flow rate of 299.37 g/min. (Adalarasan Ramalingam, 2015)

Vijay and Choudhury studied the application of pure waterjet for enhancing surface finish of machined part by abrasive waterjet. The first part of the research was observed on surface roughness and depth cut of the machined Ti-6Al-4V alloy. From Figure 2-13, it was found that as traverse speed increases, depth of cut also increases rapidly because high traverse speed allows less exposure time on machined area. The depth of pocket is high for increasing pressure and kinetic energy as depicted in Figure 2-13. There is a slight effect of waterjet standoff distance on the value of depth cut because the jet losses some kinetic energy beyond a certain value of standoff distance.

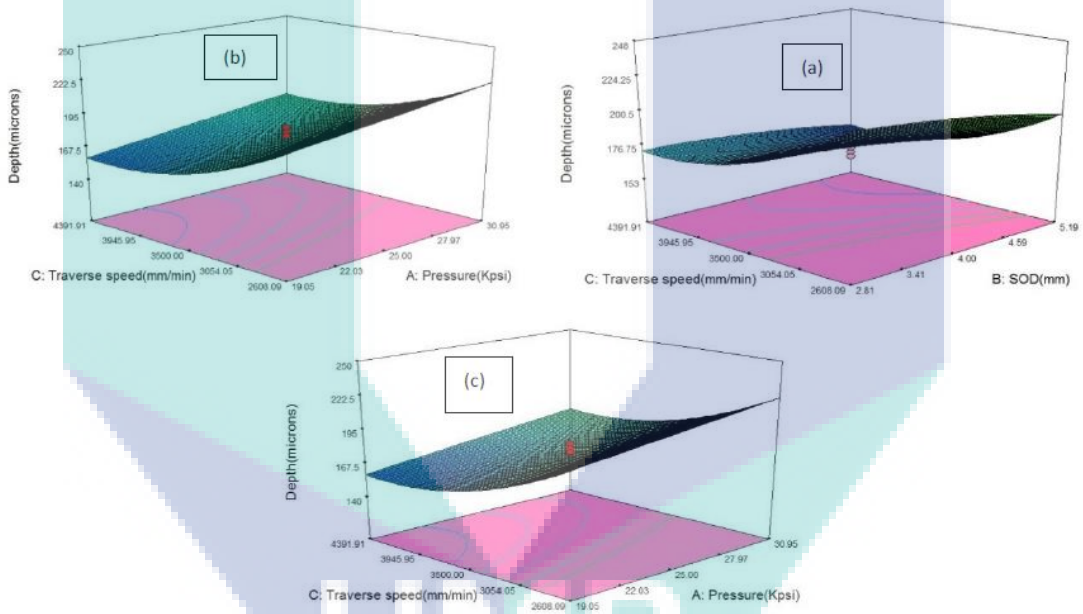

Figure 2-13 Response surface plot for (a) Stand Of Distance and Traverse Speed, (b) Pressure and Traverse Speed and, (c) Pressure and Traverse Speed for cutting Ti-6Al-4V alloy by using abrasive waterjet machining for depth cut.

Source: (Pal & Choudhury, 2014).

From Figure 2-14, it was found that high traverse speed results in high surface roughness value due to less number of abrasive particles eroding the surface area; thus creating rough surface. Rough surface occurs at high traverse speed and low pressure since this combination results in non-sufficient kinetic energy on the machined surface for smooth fracture. At larger standoff distance, surface roughness increases but needs

sufficient jet kinetic energy. This condition is clear at large pressure since the loss of energy at high standoff distance is compensated by high pressure. In addition, it is noted that there is significant effect of surface finish at high pressure and low traverse speed.(Pal & Choudhury, 2014)

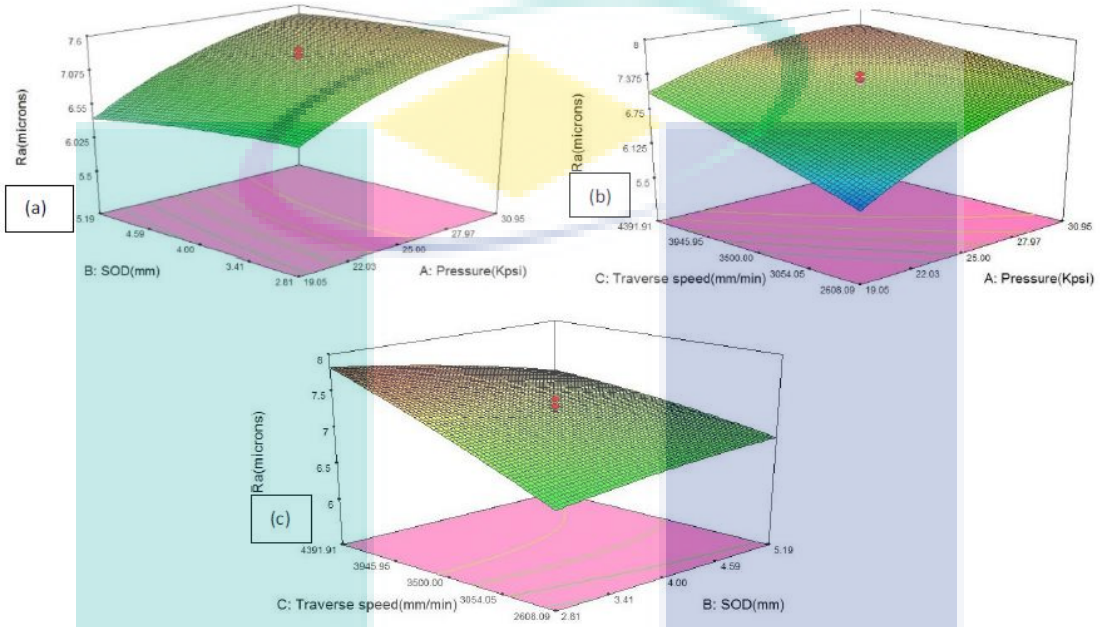

Figure 2-14 Response surface plot for, (a) Pressure and Stand Of Distance, (b) Pressure and Traverse Speed and, (c) Stand Of Distance and Traverse Speed for cutting Ti-6Al-4V alloy using abrasive waterjet machining for surface roughness

Source: (Pal & Choudhury, 2014).

Yadav and Singh investigated the influence of abrasive waterjet process parameter on surface roughness of aluminium by applying response surface method approach. They detected that traverse rate and pressure has greater significant influence on surface roughness compared to standoff distance. 3D surface shown in Figure 2-15 explains that surface quality is better as pressure is increased; meanwhile, traverse rate is elevated resulting in lower surface quality. Surface quality is poor at the beginning of machining region near the top surface at below 1 millimetre standoff distance; but surface roughness elevated at more than 2 to 3 mm standoff distance (Yadav & Singh, 2016).

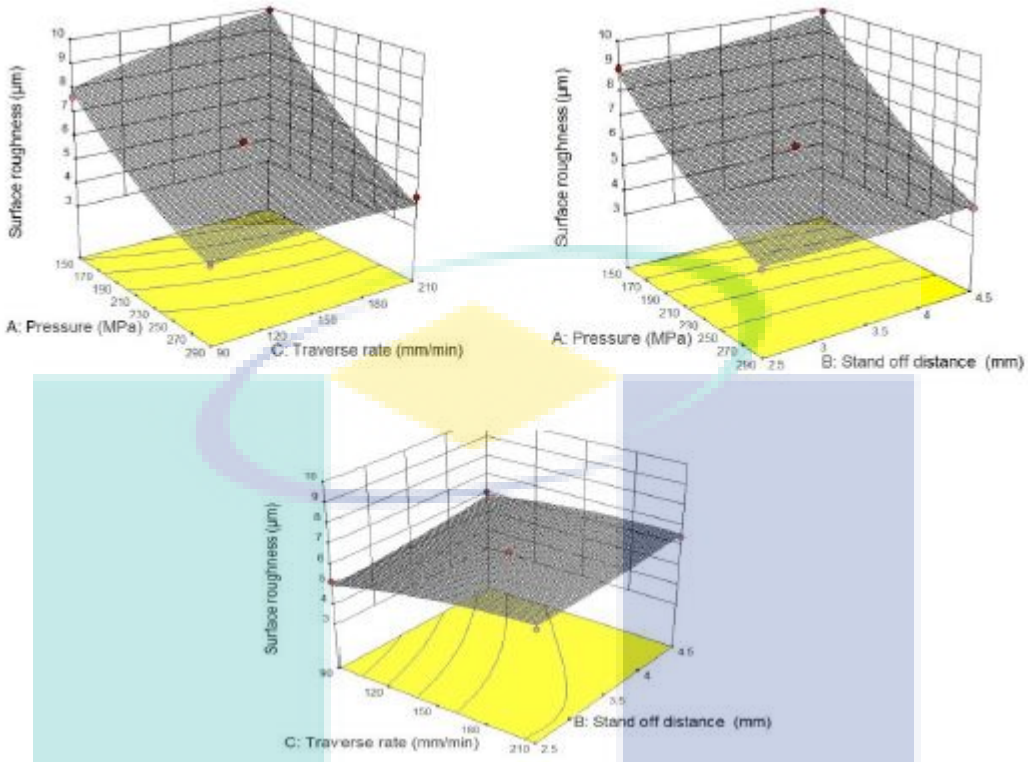

Figure 2-15 Response surface plot for interaction effect during abrasive waterjet machining of aluminium, a) pressure and traverse rate, b) pressure and standoff distance, and c) traverse rate and standoff distance

Source: (Yadav & Singh, 2016)

2.9 Summary

From the literature review, it was found that most of the studies were done focuses on the optimization to achieve the maximum paint removal with minimum substrate damage. This is consistent with the objective of the present research work which focuses on the optimization of paint removal with a new method applied in waterjet cleaning.

CHAPTER 3

METHODOLOGY

3.1 Introduction

In this section, the detailed explanation of the mechanical properties of paint, equipment used, experimental setup, introduction to water jet machine, surface roughness measurement, 3D measurement laser microscope for surface profile and method flow are presented.

3.2 Materials

Materials from a commercial automotive part were cut by mechanical saw from the original plate. The automotive part was taken from the spoiler of Perodua Alza model as shown in Figure 3-1. The material used for manufacturing the spoiler is similar for bumper of this model type. The model colour is metallic mystic purple which has aluminium flakes to enhance the beauty of the paint.

(a) (b)

Figure 3-1 (a) Automotive part from Perodua Alza (b) The processed part after mechanical sawing

Once the substrate underwent proper and primary cleaning process using dry compressed air method to take out dirt, the substrate is set to be machined. The plate was

newly acquired as it was commercial painted using various standard layers of coat. The paint on the surface of automotive plastics part has tensile mechanical properties as presented in Table 3-1(Zhang & Chen, 2015).

Table 3-1 Mechanical Properties of paint on the surface of automotive plastics component

Paint	**Elastic Modulus, *E* (GPa)**	**Yield strength, $\sigma_{0.2}$ (MPa)**	**Ultimate strength, σ_b (MPa)**
Top coating	1.59-1.76	11.34-15.85	17.43-21.22
Intermediate coating	1.54-1.88	8.99-13.10	10.71-13.75
Primer	0.52-0.77	4.93-7.11	7.83-10.60

Source: (Zhang & Chen, 2015)

Substrate used in this experiment was a commercial automotive part (spoiler/wing) which was made from polypropylene (PP). Polypropylene is widely used in automotive industry to replace engineering plastic and metal because of its capabilities to achieve weight reduction, low cost and outstanding moldability. Surface roughness test was used to measure average surface roughness of the painted polypropylene. Without any cleaning process by waterjet, the average R_a value is 0.112 µm. Thickness of the painted surface was measured by using 3D measurement laser microscope (Olympus Lext OLS5000) in 4 measurements as shown in Figure 3-2. The average thickness is calculated as in Table 3.2 below which indicates the average is 37.413 µm.

Table 3-2 Thickness measurements of automotive paint

Measurement 1	**Measurement 2**	**Measurement 3**	**Measurement 4**	**Average Thickness**
36.280 µm	37.791µm	37.791 µm	37.791µm	37.413 µm

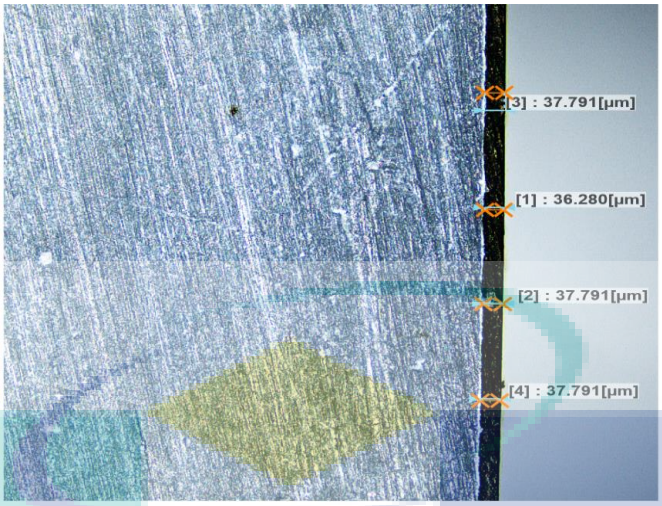

Figure 3-2 Cross sectional area of the sample with a set of paint thickness measurements selected randomly. Darker area represents paint on top of the substrate which is the paint.

3.3 Equipment

3.3.1 CNC waterjet machine

A self-developed waterjet machine was used to measure the whole experiment operation. Due to its low cost, present developed waterjet machine can produce water pressure up to 100 MPa. An air driven liquid pump is the type of pump used to generate the pressure. Computer numerical control (CNC) system was also attached to the waterjet system to control nozzle movement. The movement was controlled along multiple axes (*X* and *Y*). It can also move in the *Z*-axis (depth) to control standoff distance. The cutting head consists of tungsten carbide focusing tube and ruby orifice with diameter of 0.127 mm. The diameter of focusing tube is 0.76 mm and the length is 76.2 mm. Whilst, self-developed CNC waterjet machine is presented in Figure 3-3; cutting head assembly is shown in Figure 3-4.

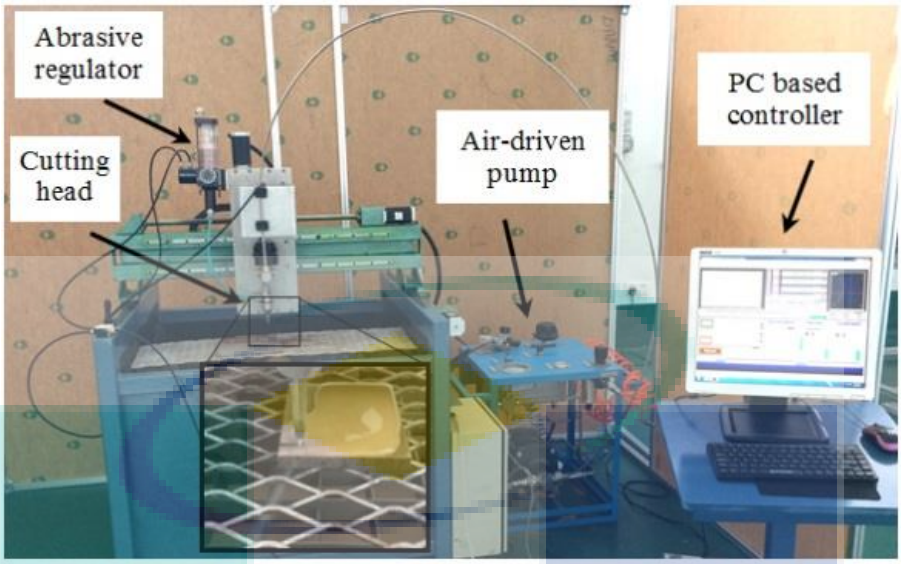

Figure 3-3 Self-developed CNC waterjet machine

Source: (Murugan, Gebremariam, Hamedon, & Azhari, 2018)

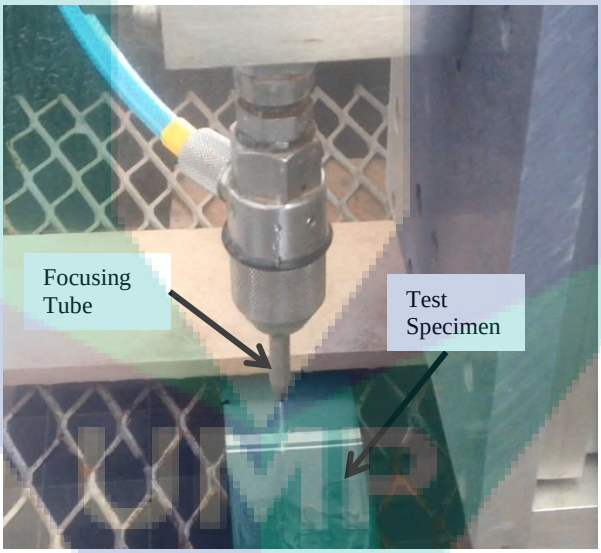

Figure 3-4 Test specimen during the paint removal process

3.3.2 Surface roughness tester

Morphological change of sample surfaces is mainly determined by surface roughness test. Arithmetic mean deviation of roughness profile, (R_a) measurements for machined surface finishes was selected in this research because it is the standard default

representation of surface machined by waterjet method. Plain waterjet cleaning was used in current study which permits the value of *Ra* analysis to be applied in the methodology. Only minor inspection distance is acquired to represent the entire surface because its finish is assumed to be uniformed. Surface roughness instrument (Mahr Marsurf PS1) as shown in Figure 3.5 was used to measure surface quality of the substrate surface. The roughness tester is equipped with a cone-shaped diamond stylus having a diameter of 5 µm and a tip angle of 90°. The roughness measurement was obtained along the transverse direction of the treated surface with a cut-off length of 2.5 mm with an evaluation length of 12.5 mm according to EN ISO 4288 standard. Parameters *Ra*, the average roughness profile of five consecutive sampling distances were assessed. Their average value was computed to minimize the variability.

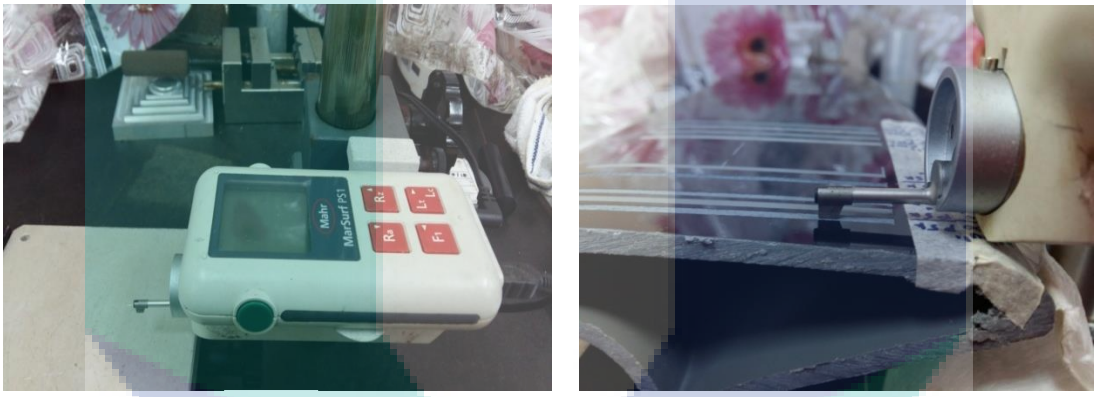

(a) (b)

Figure 3-5 (a) Surface roughness test (Mahr Marsurf PS1). (b) Direction of stylus surface roughness test runs along the cleaned surface.

3.3.3 3D Measurement Laser Microscope

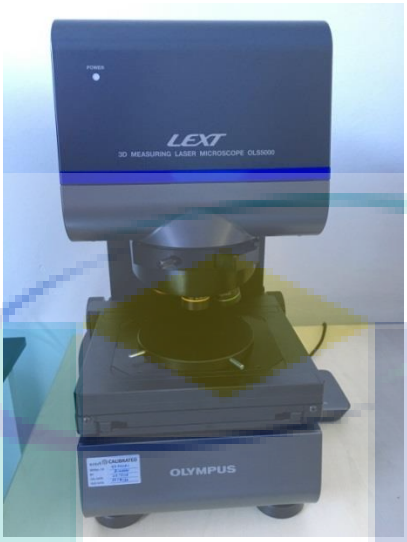

Figure 3-6 3D Measuring Laser Microscope (Olympus Lext OLS5000)

The OLS5000 laser confocal microscope is used to measure surface roughness and shape of the machined substrate at submicron level. It is able to make accurate 3D measurements with wide ranges of sample type. Simple analysis function such as measuring line width, step, area, volume and surface roughness for identified measurement area can be performed.

3.4 Experimental Procedure

Paint on automotive part surface was eroded by multiple passes of waterjet cleaning with a set of waterjet parameters setup. The waterjet machine operated with orifice size of 0.127 mm diameter and impact angle of 90° which were kept constant. The setup of cleaning parameters and their levels used in the present research are presented in Table 3-3.

Table 3-3 Machining parameters and their levels

Machining Parameters	Levels
Number of passes, *n*	1, 3
Traverse rate, *u* (mm/min)	500, 1000
Pressure, *p* (MPa)	34, 69
Stand-off distance, *s* (mm)	10, 20
Lateral feed, *f* (mm)	0.2, 0.6

Surface of free embedded abrasive particles is predicted since the operation involved plain waterjet which purely uses water as the cleaning medium. The sample was cut to small dimension from the whole component to produce flat workpiece. The surface dimension was approximately 100 mm × 100 mm and was appropriately clamped on the waterjet machine table. As shown in Figure 3-7, setup parameters for the sample were cleaned along its width. To attain coverage of cleaning area about 70 mm × 5 mm, waterjet nozzle was moved according to NC code in *y*-and *x*-directions. Apart from that, the coverage area was cleaned with successive overlapped water-generated impacts as the nozzle was moved along the sample width. With overlapping rate or lateral feed about 0.2 and 0.6 mm, satisfactory uniformity of waterjet cleaning was attained.

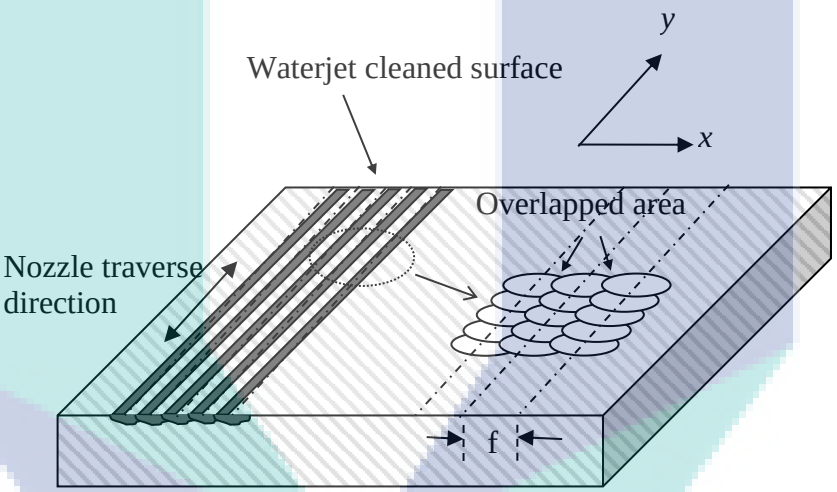

Figure 3-7 Schematic of waterjet paint removal process

3.5 Design of experiment

3.5.1 Preliminary experiment

The parameters were selected based on Response Surface Method (RSM). After important parameters or factors were identified, the levels for these factors were determined according to optimal response value or minimum magnitude of surface roughness. This was carried out through preliminary experiment as presented in Table 3.4.

Table 3-4 Experimental layout for preliminary experiment

Run	Factor 1: *p*(MPa)	Factor 2: *u*(mm/min)	Factor 3: *n*(pass)
1	34	1000	3
2	34	500	3
3	34	1000	1
4	69	500	1
5	69	1000	1
6	34	500	1
7	69	500	3
8	69	1000	3

3.5.2 First Order model

Design Expert© 7th Edition software was selected to analyse the factor which initially underwent the first order regression model using fractional two-level factorial design analysis. As shown in Table 3-5, according to two-level factorial design, 16 experimental trials were executed from the software as the main experiment.

Table 3-5 Experimental layout of two level factorial

Run	Factor 1: *p* (MPa)	Factor 2: *u* (mm/min)	Factor 3: *s* (mm)	Factor 4: *n*(pass)	Factor 5: *f* (mm)
1	34	1000	10	1	0.2
2	34	1000	20	1	0.6
3	69	1000	20	3	0.6
4	34	500	10	3	0.2
5	34	500	20	3	0.6
6	69	500	10	3	0.6
7	69	500	10	1	0.2
8	69	1000	20	1	0.2
9	34	500	20	1	0.2
10	69	500	20	3	0.2
11	34	1000	10	3	0.6
12	34	500	10	1	0.6
13	34	1000	20	3	0.2
14	69	1000	10	1	0.6
15	69	1000	10	3	0.2
16	69	500	20	1	0.6

It is very important to set the first set of experiment trials with the lowest experiment ran to achieve more efficiency in operating the experiment from current working settings to optimum section. In the process of selecting operating condition for

the following experiments, the first order model contour plot was then applied so that the process can continue to the optimum regions.

3.5.3 Second order model

Once significant parameter/factor was identified, the second order model was developed using Central Composite Design (CCD). The CCD approach is known as two-level full factorial (2^k) design which consists of centre point and other selected experiment trials. The design operation began by estimating the entire main regression parameters to fit second order model to pre-determined response. Based on the CCD approach, 13 experiments run were executed from the software as shown in Table 3-6. From these 13 runs, only one run was chosen as the optimum parameter that minimized surface roughness.

Table 3-6 Experimental layout of central composite design and its corresponding observed values of surface roughness

Run	Factor 1: *p* (MPa)	Factor 2: *f* (mm)	Response 1: R_a (µm)
1	35.3	0.7	4.754
2	33.6	0.5	5.504
3	34.0	0.6	5.983
4	32.8	0.6	2.655
5	34.0	0.6	5.983
6	34.0	0.6	5.983
7	36.2	0.6	6.404
8	34.0	0.4	7.729
9	33.6	0.7	3.259
10	35.3	0.5	8.234
11	34.0	0.6	5.983
12	34.0	0.6	5.983
13	34.0	0.8	2.104

3.5.4 Validation test

Finally, the chosen optimum parameter was repeated to check the validity of response and results. Summary of the experiment in form of flowchart is shown in Figure 3-8.

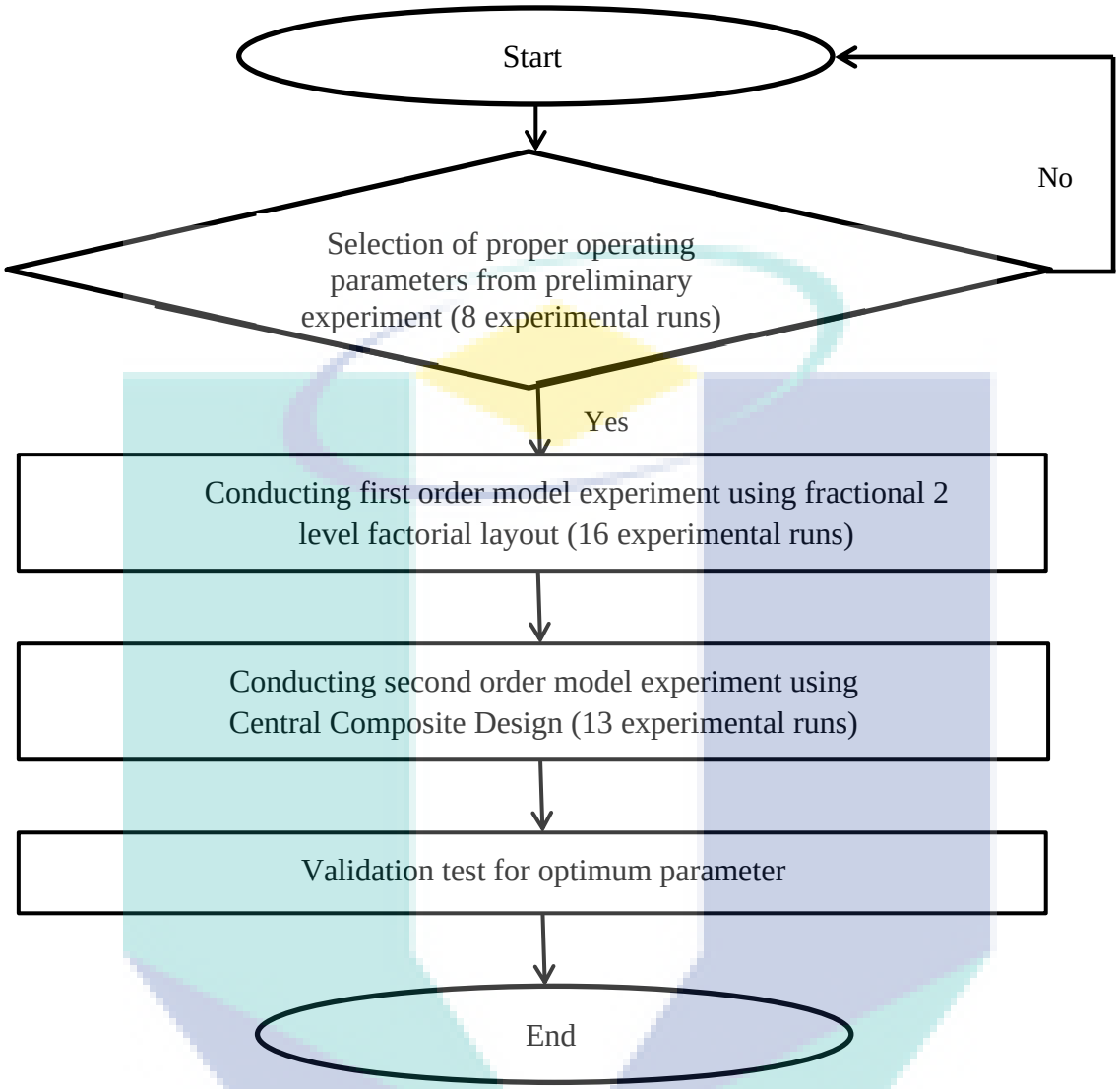

Figure 3-8 Flowchart of the experiments using waterjet paint removal process

3.6 Summary

In this chapter, the properties of the material had been analysed, the suitable equipment with its specification had been identified, the machine for surface analysis are chosen and the finalize methodology flowchart had been selected based on the objectives of the present research work.

CHAPTER 4

RESULTSAND DISCUSSION

4.1 Introduction

This chapter summarized all results on surface roughness data obtained and discuss the findings. The visual inspection and surface topography are also presented. Optimization process through 2 level fractional factorial and central composite design achieve the optimum waterjet parameter with the chosen range of data.

4.2 Results on Preliminary experiment

4.2.1 Effect of traverse rate on surface roughness

Figure 4.1 shows the effect of traverse rate on the roughness of automotive paint during waterjet cleaning at pressures of 34 MPa and 69 MPa. It was noted that adding a number of passes shows slight decrease in surface roughness except at traverse rate of 1000 mm/min with pressure of 34 MPa. This is due to smoothening action by second and third cleaning passes on the precedent surface to erode irregular surface left by previous cleaning pass similar to that multi passes cutting (Wang & Guo, 2003). Furthermore, increasing traverse rate shows moderate low surface roughness as presented in Figure 4.1. Usually, clean erosion operation with smooth surface finish is achieved by applying low traverse rate (Folkes, 2009). Moreover, minor interaction between paint coating and water particle is observed at high traverse rate (Tanmay Tiwari et al., 2018). Consequently, the waterjet manages to eliminate paint surface without damaging much of the substrate material; thus, producing flat original surface with lower surface

roughness value. In fact, it can be seen that significant high surface roughness is present as waterjet pressure increases for both single and triple cleaning passes. This is because kinetic energy of the particles soars at high pressure; thus. eroding more materials similar to the cutting materials such as stainless steel, polymeric composite materials and ceramic (Tanmay Tiwari et al., 2018).

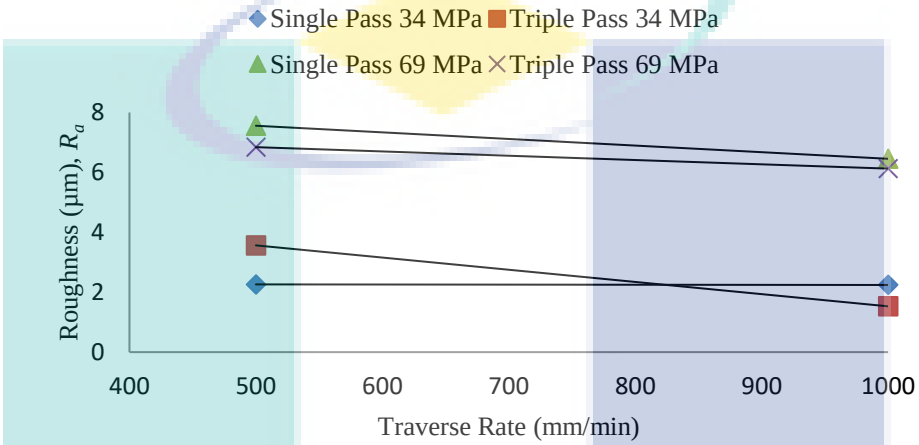

Figure 4-1 Effect of traverse rate on surface roughness for different cleaning passes and pressures

4.2.2 Effect of pressure on surface roughness

Figure 4.2 illustrates the effect of pressure on surface roughness of the painted surface at the pressure of 34 MPa and 69 MPa. It was noticed that adding a number of passes shows significant high surface roughness which is indicated by high value of gradient in the graph. For all cleaning passes, it can be observed that high surface roughness is present at high waterjet pressure. This is because increasing waterjet pressure produces high kinetic energy of water particles; therefore, eroding more materials similar to cutting ceramic (Tanmay Tiwari et al., 2018)

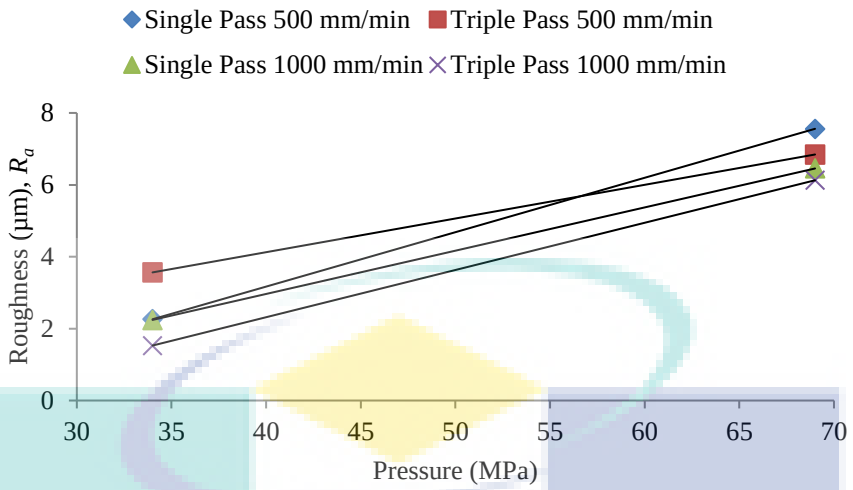

Figure 4-2 Effect of pressure on surface roughness for different cleaning passes and pressures

4.2.3 Visual Inspection for preliminary experiment

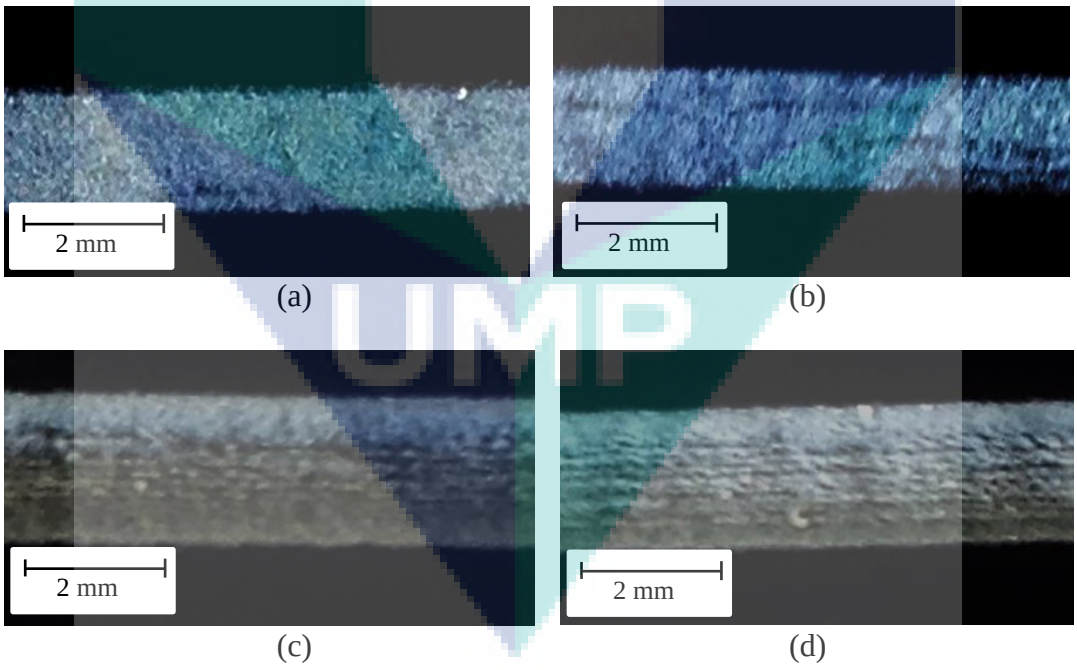

Figure 4-3 Visual effect of paint removal using single pass at different traverse rates and pressures, (a) u = 500 mm/min, p = 34 MPa (b) u = 1000 mm/min, p = 34 MPa (c) u = 500 mm/min, p = 69 MPa (d) u = 1000 mm/min, p = 69 MPa

Figure 4-3 shows visual effect of paint removal operation by using single cleaning pass at various pressures and traverse rate. In Figure 4-3 (a), (b), (c), and (d) it can be observed that some painted area is not eroded proven by the existence of black area / lines in the image. As displayed in Figure 4-4, cleaning paint at lower waterjet pressure of 34 MPa creates smoother surfaces compared to cleaning paint at higher waterjet pressure of 69 MPa. It appears that waterjet pressure of 69 MPa is too high; whereby it does not only erode the paint but some portions of the substrate as shown in Figure 4-4 (c) and (d). Furthermore, increased traverse rate produces less paint removal due to less number of water particles to erode automotive paint surface area as nozzle speed is elevated.

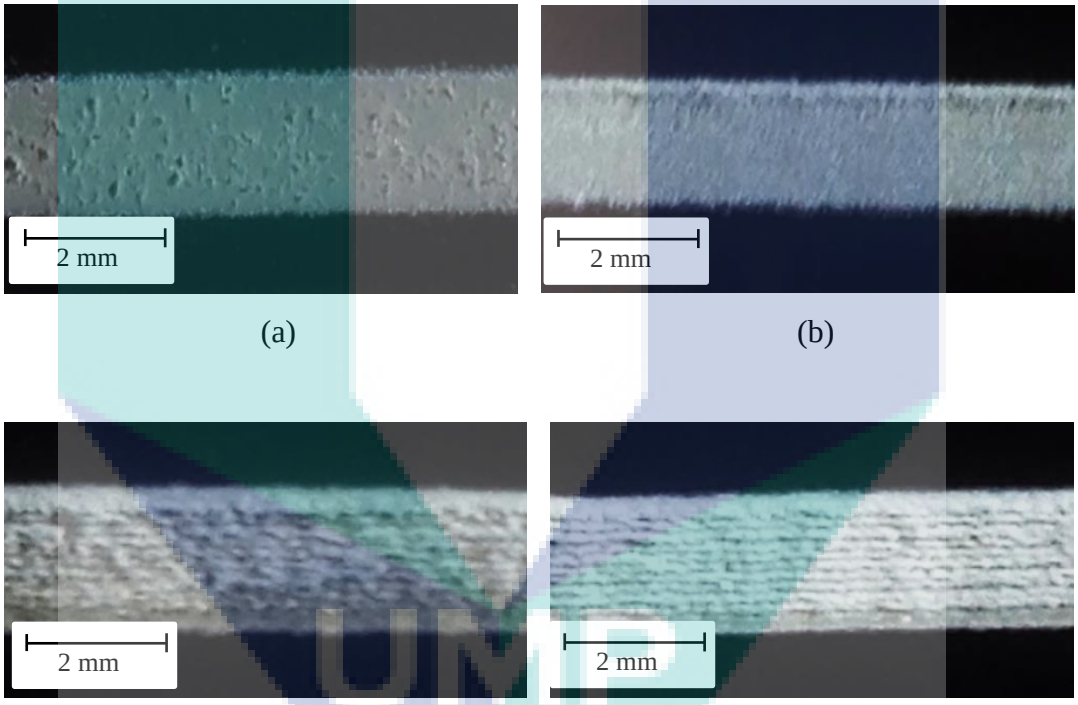

Figure 4-4 Visual effect of paint removal using three passes at different traverse rates and pressures, (a) u = 500 mm/min, p = 34 MPa (b) u = 1000 mm/min, p = 34 MPa (c) u = 500 mm/min, p = 69 MPa (d) u = 1000 mm/min, p = 69 MPa

Figure 4-4 shows the effect of paint erosion using three passes at various pressures and traverse rates. Similar deductions can be established concerning the effect of pressures and traverse rate as paint removal using single cleaning pass as shown in Figure 4-3. Besides, by comparing both Figure 4-3 and Figure 4-4 for single and three passes respectively, it can be observed that three cleaning passes erode more paint coating than

single cleaning pass. This is proved by lack of black area/ lines in the image. It seems that continuous paint removal process at every cleaning pass is the reason for the lack of black area/lines.

4.3 First order model – two-level fractional factorial design

By using two-level factorial design, all results on surface roughness from the main experiment were analysed. Through a reduced model of the factorial design, result of the first optimization is also presented. The identification of possible factors that is effective in minimizing surface roughness of automotive parts surface was carried out using 2^{5-1} fractional factorial design as shown previously in Table 3-5. This method was applied to identify the effect of the factors on response analysed in the study. Waterjet pressure, traverse rate, stand-off distance, number of cleaning passes and lateral feed were the independent factors investigated to examine its effects on surface roughness. In the study, it was found that surface roughness, R_{as} ranges from 2.85 to 7.57 μm.

4.3.1 Mathematical Model from two-level factorial

After the exclusion of non-significant parameters (p> 0.01) from the results, the regression Equation (1) signifies the best mathematical description of the response. The coefficient involved in the equation was calculated by Design Expert software. Final empirical models in terms of actual parameters were presented in terms of actual parameters as shown in Equation (1).

$$R_a = 12.89625 - 0.000836175p + 0.00453950u - 0.35727s + 0.47644n - 18.43813f - 0.000000542300pu + 0.000048675ps + 0.00169912pf \quad (1)$$

The experiment versus predicted surface roughness value calculated by using Equation (1) is presented in Figure 4.5. In Figure 4.5, it is illustrated that linear distribution graph means that well-fitting model was established. The values predicted from Equation (1) are close to the observed values of surface roughness of the cleaned automotive surface. The values are proven by prediction errors between 0.36% to 6.96%. Normal probability plot is in Figure 4.6 whereby approximate straight line graph defines

the residuals (difference between actual and predicted values) in normal distribution pattern.

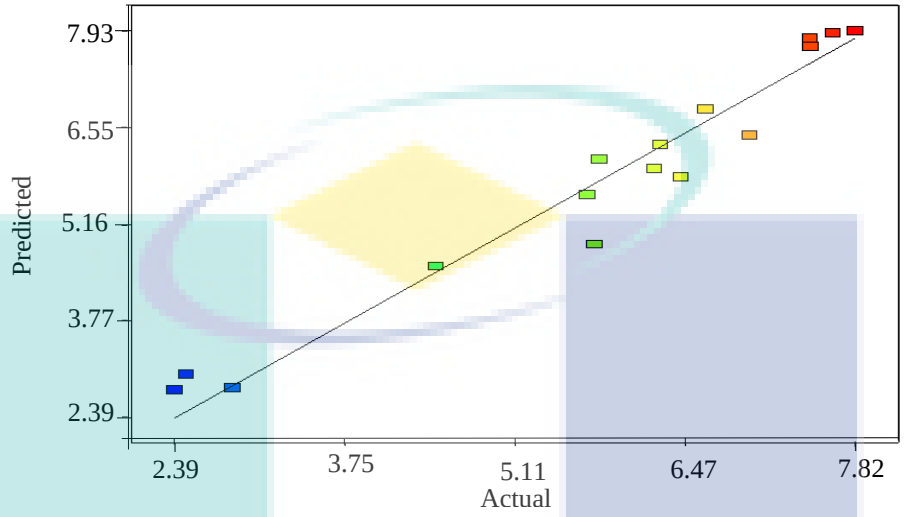

Figure 4-5 Correlation of actual conversions and values predicted by the model

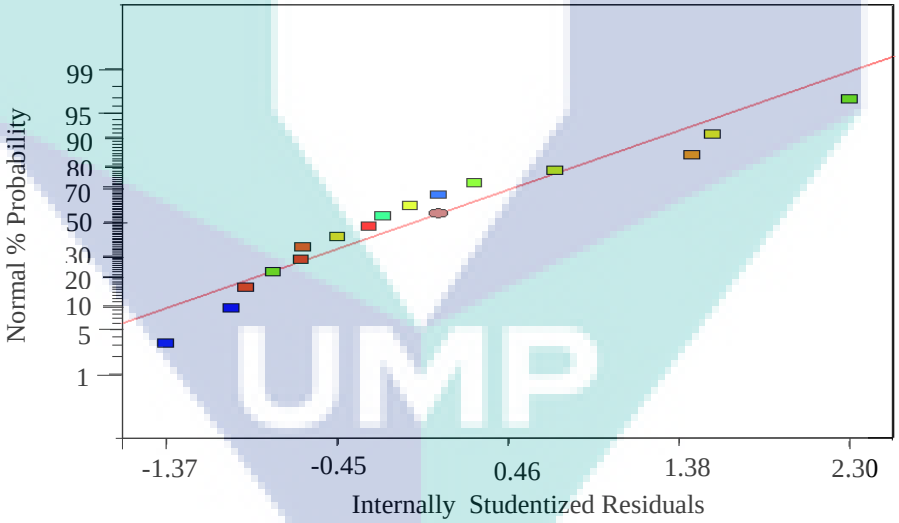

Figure 4-6 Normal probability of residual

4.3.2 ANOVA from two-level factorial

Analysis of Variance (ANOVA) is defined as an approach that applies statistical method to analyse the differences between associated parameter and their group means (Mohammed, Iqbal, & Hashemipour, 2014). Table 4-1 shows ANOVA analysis for

surface roughness to validate empirical model equation (1). Based on ANOVA analysis, independent factors are considered significance when *p*-value of main effects is less than 0.05 (Yue, Huang, & Zhu, 2014). Zhongbo Yue et al. claimed that statistically the models are significant when Prob > *F* value for the models are less than 0.05 (i.e., 95% confidence) (Yue et al., 2014). Meanwhile, coefficient of determination (R^2) is 0.9528 which shows the predicted model fulfils the experimental data satisfactorily. This indicates that the regression model can explain 95.28 % variability in the response. On the other hand, the value also proves that the model cannot be explained by only 4.72% of total variation (Hloch, Fabian, & Rim, 2008). In predicting the cleaning response of waterjet process during paint removal of automotive component, mathematical model was considered a useful representation. It is important to note that proper selection of waterjet cleaning parameters can be formulated in practical works of automotive industries. It is also essential to investigate any interaction that is significant in the experimental design analysis. The interaction of factor is discussed in subtopic 4.3.

Table 4-1 Analysis of variance (ANOVA)

Source	**Sum of squares**	***df***	**Mean square**	***F* value**	**p-value Prob >*F***
Model	46.73	8	5.84	17.65	0.0005
Pressure, *p*	2.78	1	2.78	8.42	0.0229
Traverse rate,*u*	0.22	1	0.22	0.67	0.4387
Standoff distance, *s*	0.024	1	0.024	0.073	0.7944
Number of passes, *n*	3.63	1	3.63	10.98	0.0129
Lateral feed, *f*	20.75	1	20.75	62.73	<0.0001
pu	1.84	1	1.84	5.56	0.506
ps	5.92	1	5.92	17.90	0.0039
pf	11.55	1	11.55	34.90	0.0006
Residual	2.32	7	0.33		
Cor Total	49.04	15			
Std. Dev.	0.58		*R*-Squared	0.9528	
Mean	5.77		Adj. *R*-Squared	0.8988	
C. V. %	9.97		Pred *R*-Squared	0.7533	
PRESS	12.10		Adeq Precision	11.949	

4.3.3 Percentage contribution of each factor from two-level factorial

Figure 4-7 shows pareto chart that illustrates the main effect of factors investigated in the system. It is important to note that the pareto chart is used to determine the amount and significant effects. Factor *p*, *u*, *s*, *n* and *f* represent pressure, traverse rate, standoff distance, number of pass and lateral feed respectively. The bar lengths are

proportional to the absolute value of the estimated effects with 99% confidence level according to pareto's chart method. The bar indicates the influence of the magnitude to the effects. These magnitudes are organized from left to right indicating the largest value to the smallest which were analysed from the obtained results. It is interesting to conclude that lateral feed shows the most significant effect on surface roughness in cleaning automotive paint using waterjet method. The interaction of pressure and lateral feed, interaction of pressure and number of passes, effect of pressure and number of passes are significant above *t*-value limit; whereas the effect of interaction between pressure and traverse rate is at *t*-value limit. The effects of traverse rate and standoff distance are not significant.

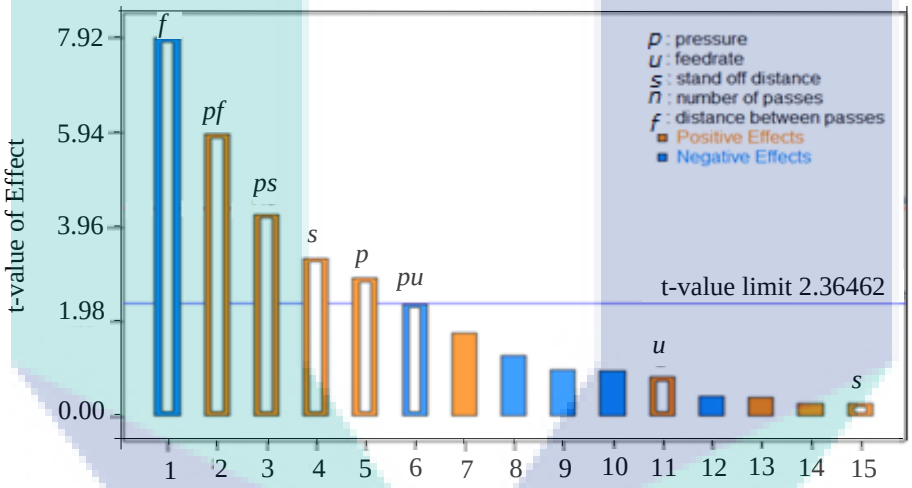

Figure 4-7 Pareto's chart of standardized effects for variables using the responses

4.3.4 Interaction between factors from two-level factorial

In interaction graph, slope of interaction plot demonstrates the relative strength of effect of the factors on the response. Interaction is possible when parameter impact depends on the second parameter setting. Cross intersection in the middle indicates strong interaction between the two factors (Tambe, 2008). Generally, the interaction of pressures with standoff distance and traverse rate in the following plots shows strong interactions. Meanwhile, no interaction occurred between pressure and lateral feed. When strong interaction is presence, the main effect should not be interpreted without interaction effect. In this subtopic, the interaction plot or graph for surface roughness with traverse rate-pressure, standoff distance-pressure and lateral feed-pressure is deliberated.

4.3.5 Interaction Plot for Surface Roughness with traverse rate and pressure from two-level factorial

Figure 4.8 displays the interaction plot for surface roughness with traverse rate and pressure. Surface roughness level was lower for traverse rate of 500 mm/min when 34 MPa pressure was applied. Conversely, surface roughness was lower for traverse rate of 1000 mm/min when the pressure was 69 MPa; and it is similar for traverse rate of 500 mm/min and pressure 34 MPa. Whilst, higher traverse rate produces negative relationship between surface roughness and pressure; lower traverse rate shows positive relationship.

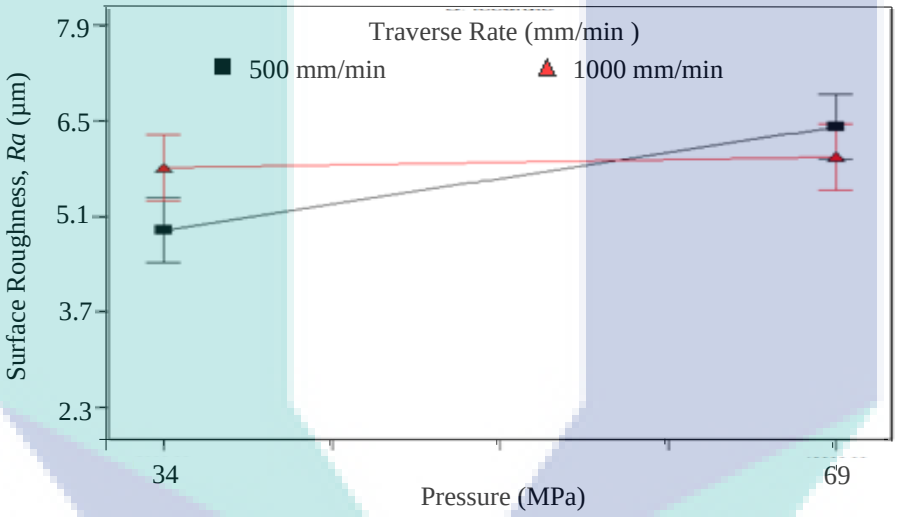

Figure 4-8 Interaction plot for surface roughness with traverse rate and pressure

Similar research by Radovanovic (2017) found that high surface roughness is shown as pressure increases at double traverse rate in machining carbon steel by abrasive waterjet,. He also detected that the interaction pressure-traverse rate result and overall effects on surface roughness is 25.94%. In this investigation, minimizing surface roughness results in high traverse rate for the increased waterjet pressures.

4.3.6 Interaction Plot for Surface Roughness with standoff distance and pressure from two-level factorial

Figure 4.9 demonstrates the interaction plot for surface roughness with standoff distance and pressure. Surface roughness is at minimum level for standoff distance 10 mm and pressure 69 MPa, or standoff distance 20 mm and pressure 34 MPa. There is

positive effect between surface roughness and pressure for high standoff distance while negative effect for lower standoff distance. An opposite finding was found by Radovanovic (Radovanovi, 2017) where negative effect of standoff distance was observed for high pressure. In addition, the interaction pressure-standoff distance effect on surface roughness was found at 3.5 % overall. In the present study, it can be concluded that to reduce surface roughness, lower standoff distance must be used for different pressures to remove the paint.

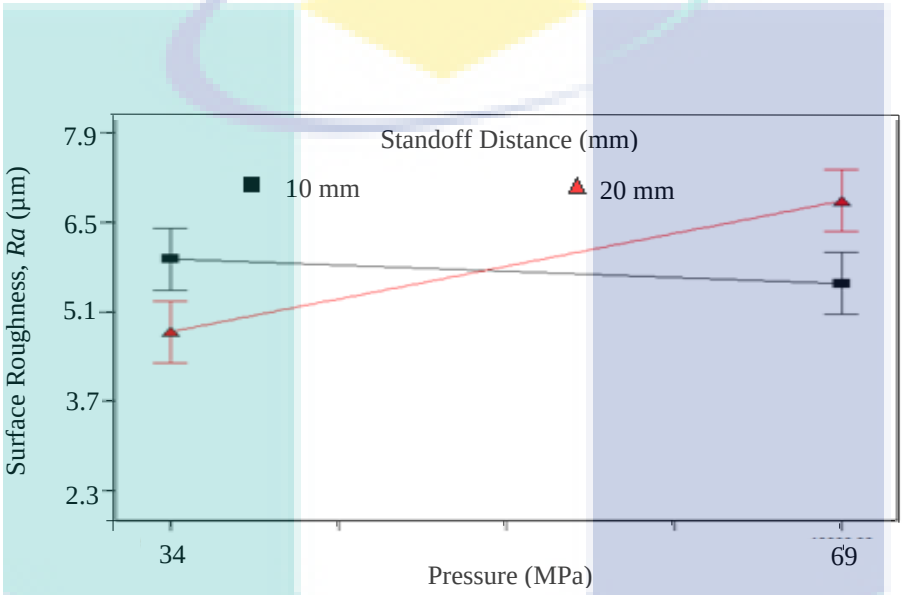

Figure 4-9 Interaction plot for surface roughness with standoff distance and pressure

4.3.7 Interaction Plot for Surface Roughness with the lateral feed and pressure from two-level factorial

Figure 4.10 demonstrates the interaction plot for surface roughness with lateral feed and pressure. It can be seen that there is no interaction between pressure and lateral feed since there is no crossing in the graph for both lines. This shows that pressure variation does not affect the magnitude of surface roughness by lateral feed variation. Lateral feed correlates with jet nozzle diameter, cut width and jet overlapping area. As lateral feed increases, width of paint removed area also increases but the percentage of jet overlapping area decreases. When the jet removes paint for the same area repeatedly after several passes, deeper cut was produced indicating the removal of material surface or substrate. A deeper cut results in high surface roughness as it damages the surface texture. (Wang, Kuriyagawa, & Huang, 2003) J. Wang et al. found that to reduce total depth of cut, jet energy impinging on the material needs to be reduced by increasing

standoff distance. Since both standoff distance and lateral feed parameters increase surface width, overlapping jet action is reduced. Hence, giving smoother surface and small depth of cut.

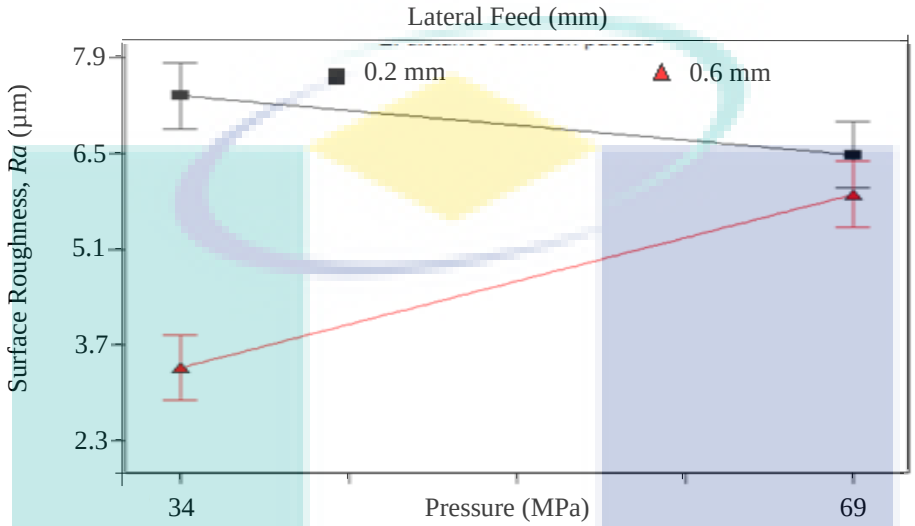

Figure 4-10 Interaction plot for surface roughness with lateral feed and pressure

4.3.8 Effect of the parameter on surface roughness from two-level factorial

In this section, effects of parameters on surface roughness are discussed. In summary, all parameters show positive effects on surface roughness; whereas lateral feed demonstrates negative effects on surface roughness.

4.3.8.1 Effect of pressure on surface roughness

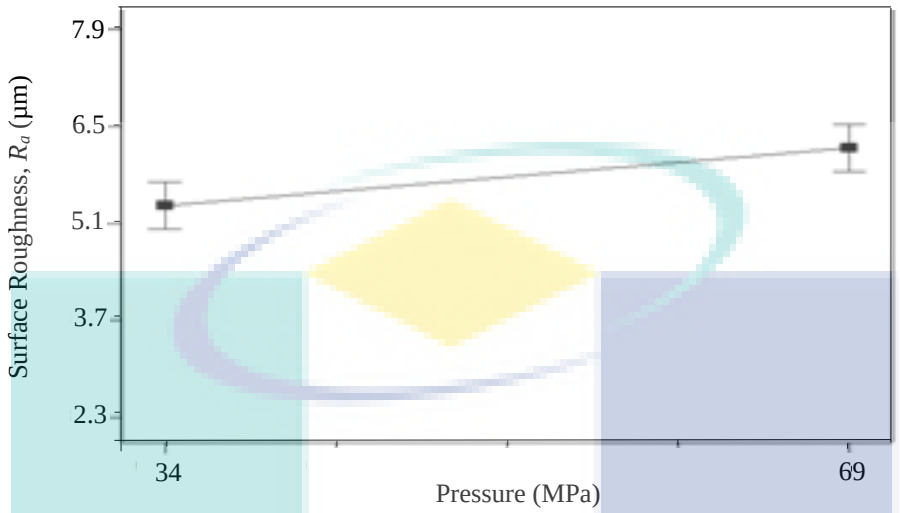

Figure 4-11 Effect of pressure on Surface Roughness

Figure 4-11 displays the effect of pressure on surface roughness. It was observed that high pressure results in high surface roughness. Kinetic energy of the water particles increases as pressure increases which results in erosion of more materials which is similar to cutting ceramic (Tanmay Tiwari et al., 2018). Azmir et al. (2013) found similar effect in machining aluminium alloy 5005; whereby surface roughness increases with high pressure. They found that surface roughness is tripled at double pressure from 50 MPa to 150 MPa. In present study, doubling the pressure from 34 to 69 MPa leads to a rise of surface roughness about 10 % from 5.45 to 6.15 µm. They determined that the increased surface roughness is due to high water supply pressure and impingement speed of water droplet. This increment may increase the jet kinetic energy; therefore, improving the material erosion ability. As a result, material surface may experience more erosion and roughness (Azhari et al., 2013).

4.3.8.2 Effect of standoff distance on surface roughness

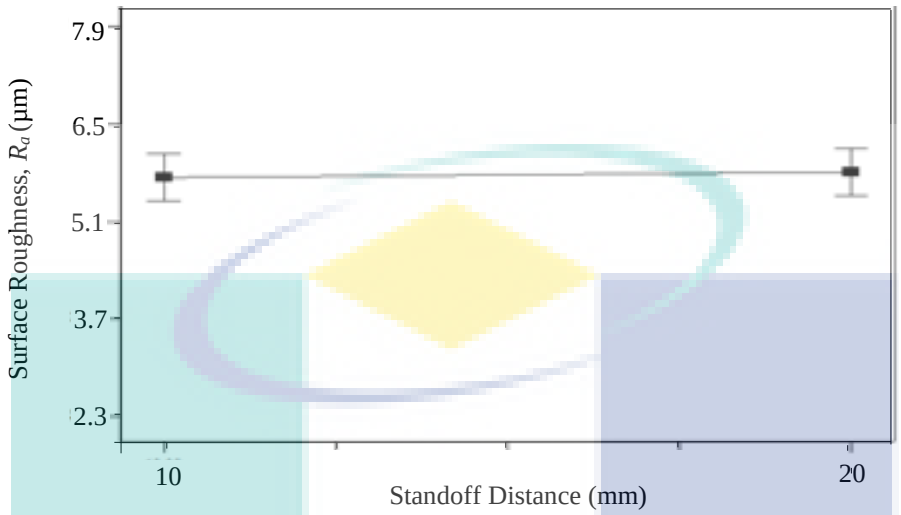

Figure 4-12 Effect of standoff distance on Surface Roughness

Figure 4-12 displays the effect of standoff distance on surface roughness. It was observed that surface roughness shows almost no change to high standoff distance from 10 to 20 mm. In contrast, Azmir et al. (2013) obtained increased standoff distance resulting in high surface roughness while machining aluminium alloy 5005. They established that surface roughness rises by half at triple standoff distance from 20 to 60 mm. They suspected that high reflection tendency of water molecules interrupts new arriving water droplets coming from the nozzle. But, at greater standoff distance they found that water molecule reflection decreases due to the spreading of water. They concluded that maximum removal rate is present at greater standoff distance before erosion rate decreases (Azhari et al., 2013). Oka et al. found that at low standoff distance, low removal rate is present as water droplets are not produced; instead water column or waterjet continuous beam is generated. This beam only presses the workpiece surface without applying cyclic stresses. Thus, the impact frequency of water is too small to generate high material removal at low standoff distance (Oka, Mihara, & Miyata, 2007). In the present study, it can be deduced that increased standoff distance shows insignificance change in surface roughness. This is possibly because their difference between the maximum and minimum distances is not high at only 10 mm. This occurs because water column is only emitted at this standoff distance (< 20 mm). Thus, less paint is removed without eroding the substrate material.

4.3.8.3 Effect of traverse rate on surface roughness

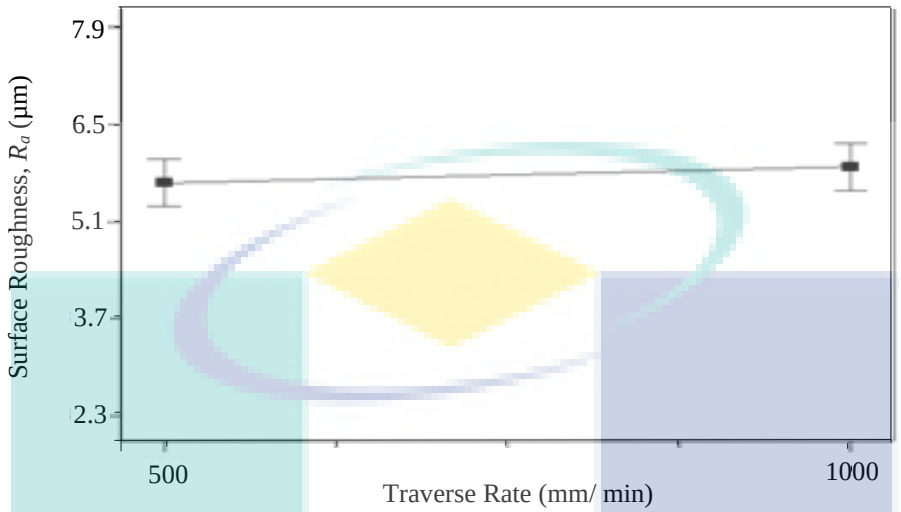

Figure 4-13 Effect of traverse rate on surface roughness

Figure 4-13 displays the effect of traverse rate on surface roughness. An increased traverse rate generates rougher surface as shown in Figure 4-13. However, the increment on surface roughness is minimal. As explained by Folkes (Folkes, 2009b) that low traverse rate generates clean removal process with smooth surface finish. Moreover, in other research, Tiwari et, al. mentioned that high traverse rate leads to high value of surface roughness due to low interaction between water particles and ceramic surface. Ineffective erosion of substrate also results in rough surface (Tanmay Tiwari et al., 2018). Wang and Guo (2003) found similar effect in machining ceramic where surface roughness is elevated with high traverse rate. They concluded that high traverse rate decreases the amount of particles impinging on the cutting front; thus, reducing smoothening action. They also observed that surface roughness increases when machining ceramic at double of traverse rate from 1 to 3.33 mm/s (Wang & Guo, 2003). Azmir et al. (2013) also obtained similar result when machining aluminum alloy 5005 whereby traverse rate is directly proportional to surface roughness. They explained that lower traverse rate results in more machining overlap actions and additional water particles collide on the surface; thus, enhancing aluminium surface roughness. They observed that surface roughness decreases by almost half during waterjet peening of aluminum at double travese rate from 500 to 1500 mm/min (Azhari et al., 2013).

4.3.8.4 Effect of number of passes on surface roughness

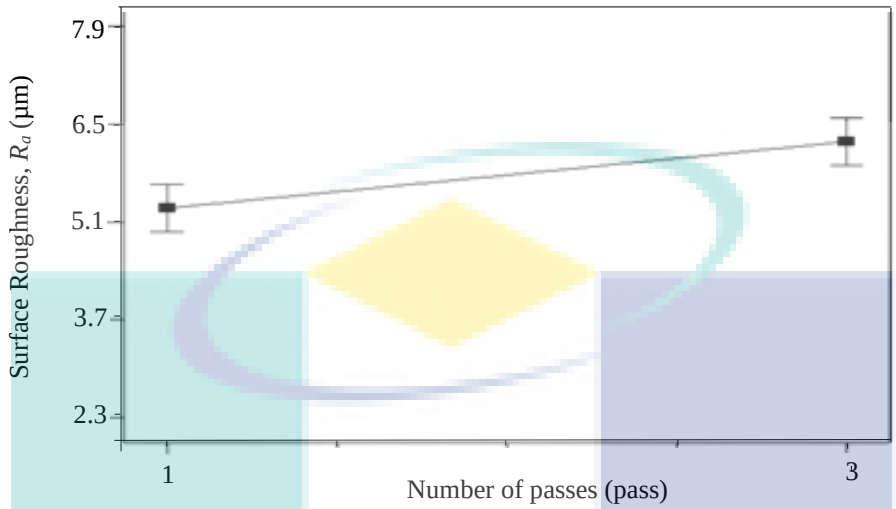

Figure 4-14 Effect of number of passes on Surface Roughness

Figure 4-14 displays the effect of number of passes on surface roughness. It was observed that increasing the number of passes results in the increment of surface roughness. In contrast, Wang and Guo (2003) found opposite result, whereby an increase in the number of passes results in a decrease of surface roughness. He suggested that smoothening action occurs by the second and third machining pass on the same surface to erode irregular surface left by precedent machining pass on the kerf wall when cutting ceramics. They also observed that surface roughness decreases by almost 40% when machining ceramic by single pass to three passes (Wang & Guo, 2003). Azmir et al. (2013) also obtained similar effect in waterjet peening of aluminum alloy 5005; whereby surface roughness elevates as number of passes increases. They found that surface roughness raises by half from single to triple passes. They concluded that subsequent passes result in smoothening action on the surface producing roughe surface. The result of rougher surface is caused by frequent bombardment of waterjet particles onto the surface substrate (Azhari et al., 2013).

4.3.8.5 Effect of lateral feed on surface roughness

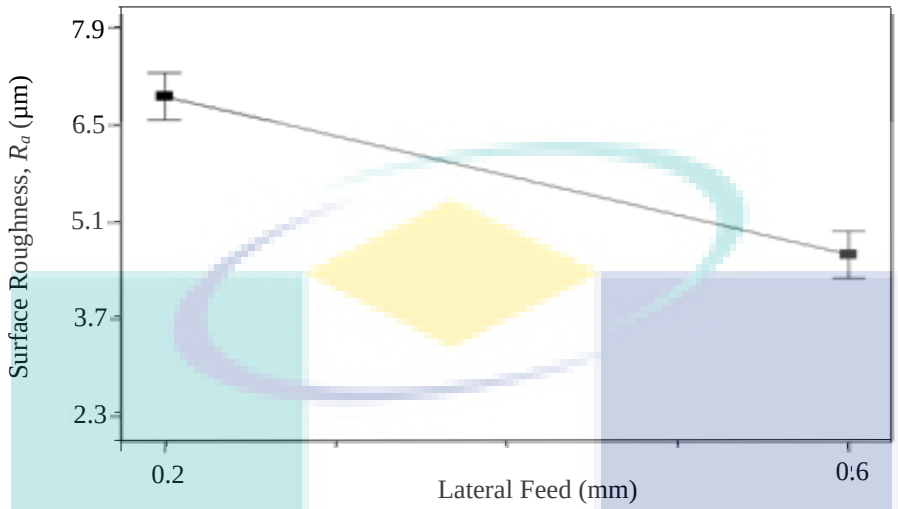

Figure 4-15 Effect of lateral feed on surface roughness

Figure 4-15 displays the effect of lateral feed on surface roughness. It was observed that high lateral feed leads to a decrease in surface roughness value. Possibly, the surface roughness is low because of less overlapping of cleaning passes at the same spot as in multiple passes. Moreover, lower impingement of waterjet droplets on the same cleaning pass resulting in less removal of paint surface; thus, reducing surface roughness value. The present study determines that surface roughness is reduced by almost half at triple of lateral feeds from 0.2 to 0.6 mm.

4.3.9 Visual observation – two level factorial

Results on the visual observation of eroded surfaces are presented based on 2D and 3D images acquired using an optical and confocal microscope respectively. Figure 4.16 displays eroded surfaces after the removal of paint for a single waterjet pass at different levels of pressure, feedrate, standoff distance and lateral feed. In general, it can be clearly seen that there are two distinct features of eroded surface with continuous erosion tracks indicated by uniform removal of paint over the whole treated region and discontinuous erosion tracks indicated by lines between the tracks or 'V' shape groove. This happened during the removal of paint using a higher lateral feed of 0.6 mm as shown in Figure 4.16 (b), (c), (e) and (h) where clear black lines indicating non-removal of paints. This is attributed to less of overlapping area as an increment in lateral feed results

in the decrement of overlapping area compared to lateral feed of 0.2 mm as shown in Figure 4.16 (a), (d), (f) and (g) with the topography of eroded surface covering the whole area by having a wavy surface with peaks and valleys. Furthermore, although the waterjet cleaning with a lateral feed of 0.2 mm has shown a more uniform erosion over the treated region however it can be noticed in some samples the presence of discontinuous cracks or non-removal of paints as indicated in Figure 4.16 (f) and (g). This tearing phenomenon caused by the waterjet action may happen due to the opposite stretching generated by the jet on target which participates the decoating process (Mabrouki & Raissi, 2002).

In case of standoff distance, it can be noticed that waterjet cleaning with a higher standoff distance of 20 mm showed a shallow penetration with small distance between peak to valley as shown in Figure 4.16 (b), (d), (f) and (h) as compared to Figure 4.16 (a), (c), (e) and (g). This relatively high standoff distance causes the divergence of waterjet thus reducing the kinetic energy of the jet (Chillman, Ramulu, & Hashish, 2016). In other word, the exposure of the jet to external drag from the surroundings at a higher standoff distance causing the waterjet to spread thus reducing the jet kinetic energy with an enlarged jet diameter (Selvan & Raju, 2012). As a result, shallower erosion tracks were formed.

In contrast, Teimourian et al. (2010) discovered that high standoff distance results in more paint loss during cleaning on steel substrate. This linear relation between standoff distance and mass loss is valid once standoff distance reaches optimum value (Teimourian, Shabgard, & Momber, 2010). Possibly, more cleaning area is produced at higher standoff distance as a result of wider impact area but with a shallower erosion tracks as found in the present study. It is also possible that the standoff distance used in the present study is above optimum value. Also, at lower standoff distance, there is a high tendency for water droplet to reflect and disturb the incoming water from the nozzle. Some water may remain on the surface after single cleaning pass. If more cleaning passes are used, more water may remain on the surface for the next cleaning passes. Therefore, the collision of reflected water droplet with incoming and existing water after first cleaning increases.

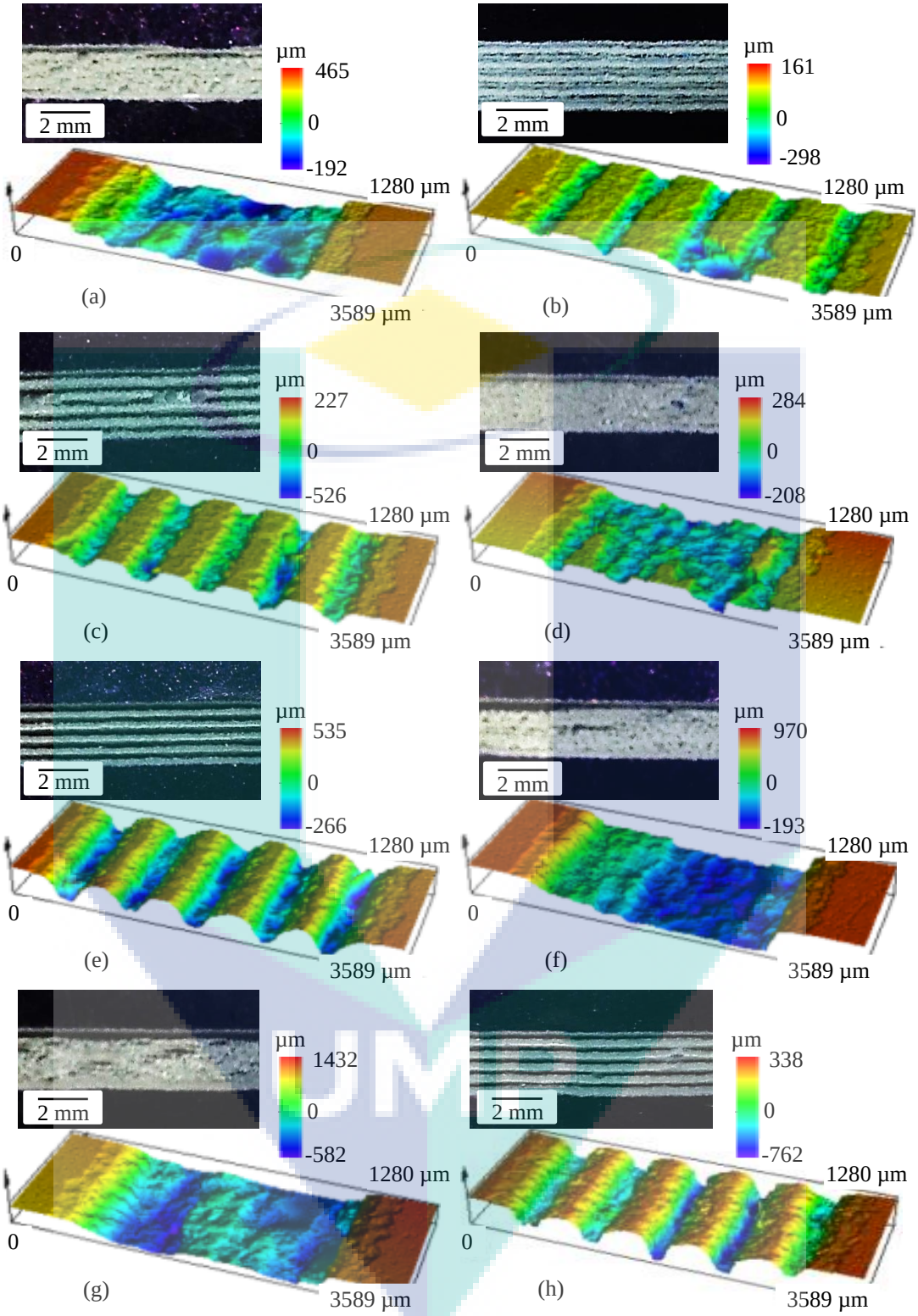

Figure 4-16 2D and 3D images for waterjet paint removal with a single pass at, (a) p = 34 MPa, u = 1000 mm/min, s = 10 mm, f = 0.2 mm, (b) p = 34 MPa, u = 1000 mm/min, s = 20 mm, f = 0.6 mm, (c) p = 34 MPa, u = 500 mm/min, s = 10 mm, f = 0.6 mm, (d) p = 34 MPa, u = 500 mm/min, s = 20 mm, f = 0.2 mm, (e) p = 69 MPa, u = 1000 mm/min, s = 10 mm, f = 0.6 mm, (f) p = 69 MPa, u = 1000 mm/min, s = 20 mm, f = 0.2 mm, (g) p = 69 MPa, u = 500 mm/min, s = 10 mm, f = 0.2 mm and (h) p = 69 MPa, u = 500 mm/min, s = 20 mm, f = 0.6 mm.

However, spreading of waterjet stream reduces the collision when standoff distance is increased for more cleaning passes (Anglani, F., Barry, J., Dekkers, W., 2017). Furthermore, Alberdi et al. (2017) concluded that there is strong relation between standoff distance and lateral feed. They found that lateral feed and standoff distance should be kept fixed to maintain the same overlap area for material removal. Figure 4.16 (b) and (d) indicate that black areas/ lines are less for a higher standoff distance of 20 mm as compared to Figure 4.16 (a) and (c) which have a lower standoff distance of 10 mm thus showing higher amount of paint removal for the former.

Also, it can be seen that the waterjet cleaning at a higher pressure of 69 MPa resulted in rougher surface with deeper erosion tracks as shown in Figure 4.16 (e), (f), (g) and (h) as compared to Figure 4.16 (a), (b), (c) and (d) with a lower pressure of 34 MPa respectively. This is attributed to a higher kinetic energy of the waterjet as pressure increases thus causing more erosion with deeper valleys. A higher pressure allows more water droplets to impinge on the cleaning area thus increasing the waterjet capability to remove more paint. Similar to the waterjet cutting process using abrasives, a higher waterjet pressure enhances the possibility of collision between particles due to the acceleration and additional energy disbursement from abrasives by the waterjet thus removing more materials and deeper erosion (Badgujar & Rathi, 2014). Furthermore, this capability allows water droplets to penetrate deeper into the cleaning area which does not only erode the paint but also damaging the substrate. It is to note the thickness of paint is less than 100 µm. Based on Figure 4.16, it can be observed that all samples experienced a certain degree of damage to the substrate with the valley of erosion tracks measuring above 100 µm. The damage to the substrate is more obvious during the waterjet cleaning of paint with a higher pressure of 69 MPa as indicated with deeper valleys.

More penetration at the cleaning area were noticed at the traverse rate of 500 mm/min as shown in Figure 4.16 (c), (d), (g) and (h) as compared to Figure 4.16 (a), (b), (e) and (f) with a higher traverse rate of 1000 mm/min respectively. A lower feedrate allows the overlapping of machining action and additional waterjet molecule to hit the target material (Azhari, Schindler, & Li, 2013). Hence, contact time between water droplets and substrate is also more. Increasing contact time by decreasing traverse rate results in more cleaning area overlapping as water droplets have more time to remove the paint area. Basically, additional overlapping action allows more water molecules from the nozzle to impinge on the same area causing rougher cleaning area. A lower traverse rate results in low nozzle speed causing water droplets to attack the surface longer. A

high traverse rate contributes to low paint erosion because small amount of water particles was used to remove surface area as nozzle speed increases. Consequently, the cleaned surface topography appears in wavy shape as peak and valley are formed.

Figure 4.17 displays eroded surfaces after the waterjet removal of paint for three jet passes at different levels of pressure, feedrate, standoff distance and lateral feed. In general, same deductions can be said concerning the effect of pressure, traverse rate, standoff distance and lateral feed when the cleaning process employed a single pass method. The major difference by comparing single and three passes, it was observed that the latter erodes more paint than the single cleaning pass as indicated by more removal of paint and deeper erosions tracks especially in Figure 4.17 (e) and (h) with the depth of valleys exceeding 1000 µm. This is due to continuous cleaning of automotive paint at every pass thus removing more material with a higher penetration. The continuity of removal process from more cleaning passes increases overlapping action and number of water molecules bombarding at the same cleaning area (Azhari et al., 2013). As a result, the erosion tracks with shapes of peak and valley formed as shown in Figure 4.16 do not appear in Figure 4.17 since additional number of cleaning passes have completely removed the shape. In other words, the subsequent jet passes eliminate the 'V' shape grooves thus producing smoother erosion track with less wavy surface. This is possibly because more cleaning passes removed the remaining paint on the surface by smoothening action same as described by Guo and Wang (2003). Figure 4.17 indicates that more cleaning passes do not only remove the paint but also causing more damage to the substrate as compared to Figure 4.16 with a smoother topography when single cleaning pass was used. However, small peaks were still formed at random along the erosion track as shown in Figure 4.17. Generally, it can be said that the paint erosion mechanism tracks are stochastic in nature. This is due to the highly stochastic nature of the plastic deformation in material surfaces thus making it difficult to produce a uniform erosion over the surface (Azhari & Schindler, 2012). Also, as previously discussed, more cleaning passes allow more water droplets to attack the same cleaning area thus enhancing the waterjet capability to remove paint as well as causing damage to the substrate material at the same time.

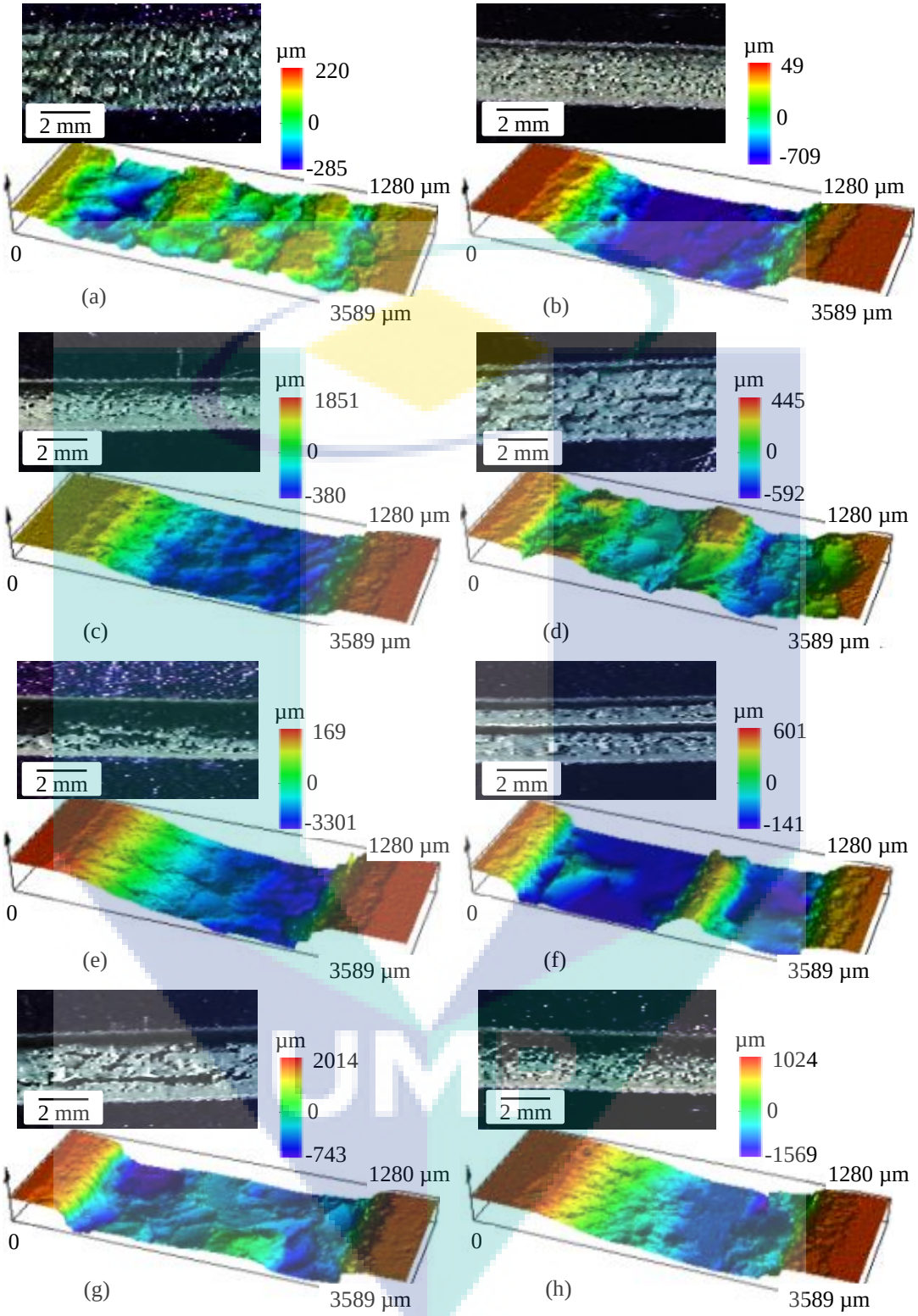

Figure 4-17 2D and 3D images for waterjet paint removal with three passes at, (a) p = 34 MPa, u = 1000 mm/min, s = 10 mm, f = 0.6 mm, (b) p = 34 MPa, u = 1000 mm/min, s = 20 mm, f = 0.2 mm, (c) p = 34 MPa, u = 500 mm/min, s = 10 mm, f = 0.2 mm, (d) p = 34 MPa, u = 500 mm/min, s = 20 mm, f = 0.6 mm, (e) p = 69 MPa, u = 1000 mm/min, s = 10 mm, f = 0.2 mm, (f) p = 69 MPa, u = 1000 mm/min, s = 20 mm, f = 0.6 mm, (g) p = 69 MPa, u = 500 mm/min, s = 10 mm, f = 0.6 mm and (h) p = 69 MPa, u = 500 mm/min, s = 20 mm, f = 0.2 mm.

4.3.10 Optimization for two level factorial design

For an optimization process, three optimal solutions were randomly selected to verify the validity of response surface equation.

Table 4-2 Optimal selection for surface roughness for higher desirability

No	*p* (MPa)	*f* (mm)	*u* (mm/min)	*s* (mm)	*n*	R_a	Desirability	Remarks
1	34.0	0.60	500	10	1	2.3732	1.000	Selected
2	34.0	0.60	500	10	1	2.3672	0.981	
3	34.0	0.60	500	10	1	2.3561	0.921	

For an optimization process, three optimal solutions were randomly selected to verify the validity of response surface equation.

Table 4-2 shows the optimum parameter after two-level factorial using response surface method (RSM) is at pressure of 34.0 MPa, traverse rate of 500 mm/min, standoff distance of 10 mm, number of passes of 1 and lateral feed of 0.6 mm.

4.4 Second order model –centre composite design (CCD)

In order to determine optimum process parameter of the main parameters, (i.e. lateral feed and pressure for minimum surface roughness), the experiments were designed in accordance to face centered central composite design in two variables following Response Surface Methodology (RSM).

4.4.1 Experimental data from CCD

The experimental set-up and corresponding experimental responses are shown in Table 3-6. Surface roughness from the samples exhibits an increment; whereby pressure decreases and lateral feed increases. Whilst, the lowest R_a value of 2.104 µm was obtained at 34.0 MPa, 0.8 mm lateral feed; the highest value R_a of 7.729 µm was obtained at 34.0 MPa, 0.4 mm lateral feed.

4.4.2 Model from CCD

The second-order polynomial models used to express surface roughness (Y) as a function of independent variables are shown in Equation 2 in terms of actual parameters.

$$R_a = -545.71978 + 0.19729p + 141.10773f - 0.024700pf - 0.0000174383p^2 - 26.32241f^2 \quad (2)$$

Overall prediction error is less than 6% which means the equation model is satisfactory. In addition, the adequacies of developed model were rechecked by Analysis of Variance (ANOVA).

4.4.3 ANOVA from CCD

Table 4-3 summarizes ANOVA (*F*-test) and *p*-value that were used to estimate coefficients of the model and significance of each parameter as well as interaction strength of each parameter. It was observed from the ANOVA analysis that confidence level is greater than 95%' while *p*-value of the model is less than 0.0001. The model with *p*-value below 0.05 is statistically significant which implies the model was suitable for this experiment. The main effects i.e. pressure and lateral feed are significant based on *p*-values.

Table 4-3 Analysis of variance ANOVA for response surface quadratic model

Source	**Sum of squares**	**df**	**Mean square**	**F value**	**p-value Prob >F**	
Model	38.64	5	7.73	26.89	0.0002	Significant
Pressure, *p*	12.25	1	12.25	42.62	0.0003	
Lateral feed, *f*	23.45	1	23.45	81.60	<0.0001	
pf	0.38	1	0.38	1.33	0.2872	
p^2	1.70	1	1.70	5.92	0.0452	
f^2	1.59	1	1.59	5.52	0.0511	
Residual	2.01	7	0.29			
Lack of Fit	2.01	3	0.67			
Pure Error	0.000	4	0.000			
Cor Total	40.65	12				
Std. Dev.	0.54		R-Squared	0.9505		
Mean	5.34		Adj. R-Squared	0.9152		
C. V. %	10.03		Pred R-Squared	0.5598		
PRESS	17.90		Adeq Precision	16.557		

The coefficient of determination (R^2) and adjusted coefficient of determination (R^2_{adj}) were 0.9505 and 0.9152, respectively which indicate that the estimated model fitted the experimental data satisfactorily. A good fit model, R^2 should be at least 0.80 (Lee et al., 2010). The R^2 for these variables was higher than 0.80 indicating that the

regression models explained the mechanism well. When the R^2 approaches value of 1, it indicates good correlation between the experimental and predicted value (Rate, Flow, & Bamboo, 2015).

4.4.4 Actual vs predicted from CCD

Figure 4.18 shows experimental versus predicted surface roughness obtained from equation (1). A linear distribution was observed which is indicative of well-fitting model. The values predicted from Equation (1) were close to the observed values of surface roughness of cleaned automotive surface. Normal probability plot is also presented in Figure 4.19. The plot indicates that the residuals (difference between actual and predicted values) follow normal distribution and form approximate straight line.

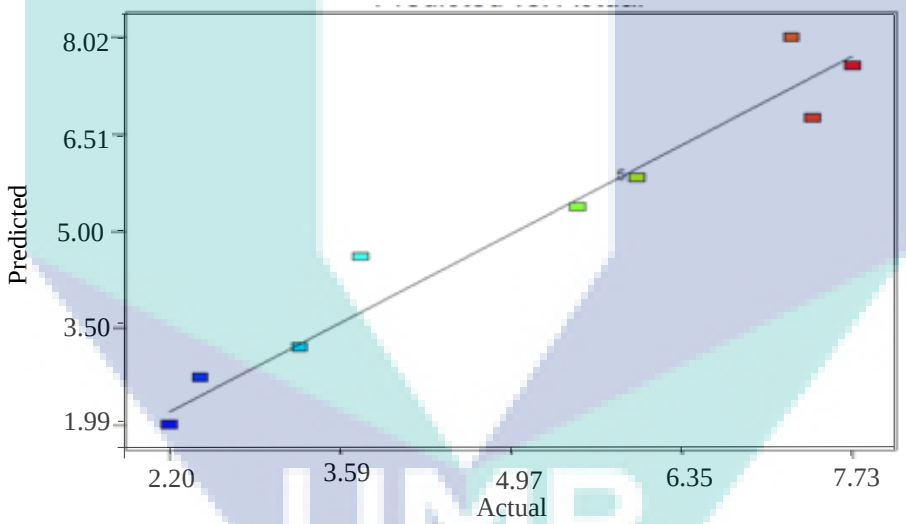

Figure 4-18 Correlation of actual conversions and values predicted by the model

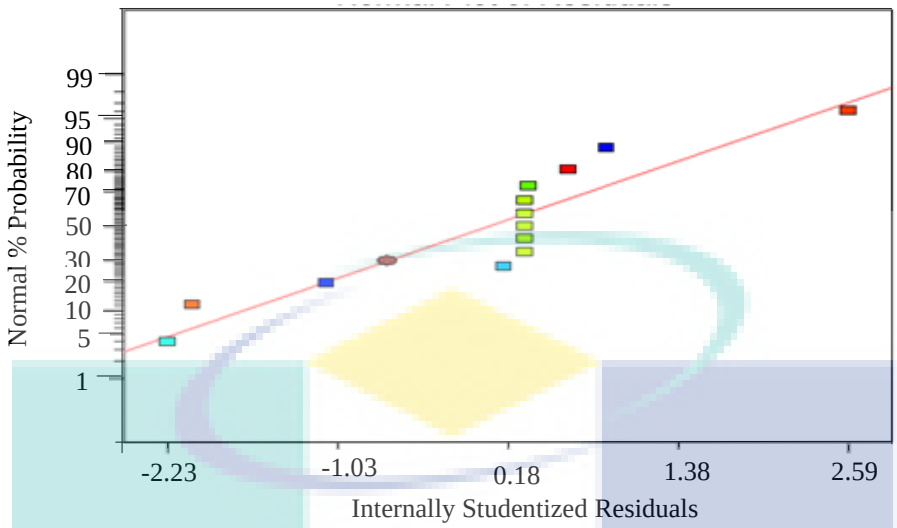

Figure 4-19 normal probability of residual

4.4.5 Effect of main parameter on surface roughness minimization from CCD

4.4.5.1 Effect of pressure on surface roughness

Figure 4-20 shows the effect of pressure on surface roughness minimization. The figure indicates that high pressure increases surface roughness of cleaned surface. This result is consistent with another study. They found that the increase of surface roughness and pressure as a result of high rate of collision between particles is caused by the elevation of energy emission from the abrasive to impact area in machining granite using abrasive waterjet (Aydin et al., 2011). In machining cast iron with abrasive waterjet, Selvan and Raju (2012) concluded that increased pressure produces smoother surface because brittle abrasives break down into smaller pieces; with the reduction of abrasive size, surface roughness decreases. In contrast, current study discovered that surface roughness is higher with increasing pressure when plain waterjet was used.

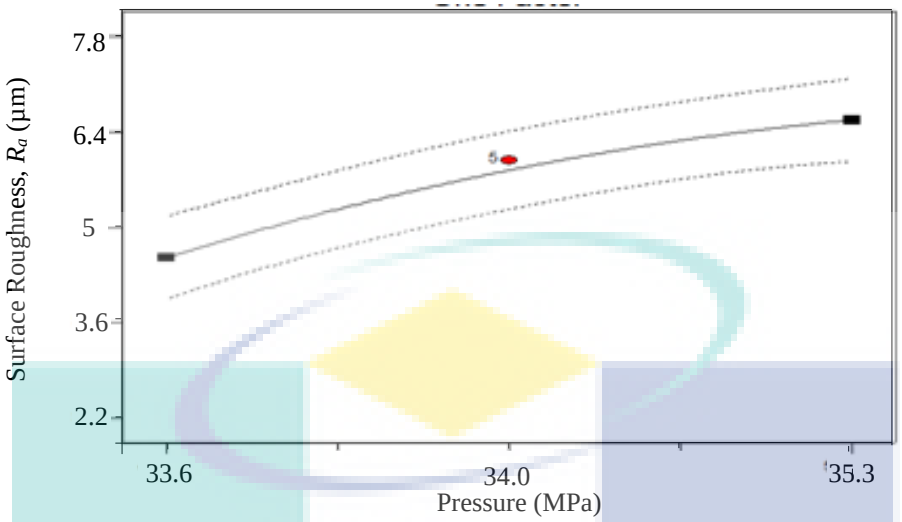

Figure 4-20 Effect of pressure on surface roughness minimization

4.4.5.2 Effect of lateral feed on surface roughness

Figure 4-21 shows lateral feed effects on surface roughness minimization. High lateral feed results in low surface roughness. From the pareto chart in previous subtopic, it was found that lateral feed has the highest significant effect on surface roughness. The lateral feed correlates with the overlapping cut area (Rivero et al., 2017). The higher the lateral feed, the lower the overlapping cut area is. It reduces the possibility of jetting impingement of water droplets on the same spot as in multiple cleaning passes. Moreover, lower impingement of waterjet droplets on the same cleaning pass resulting in less removal of paint surface thus reducing the surface roughness value.

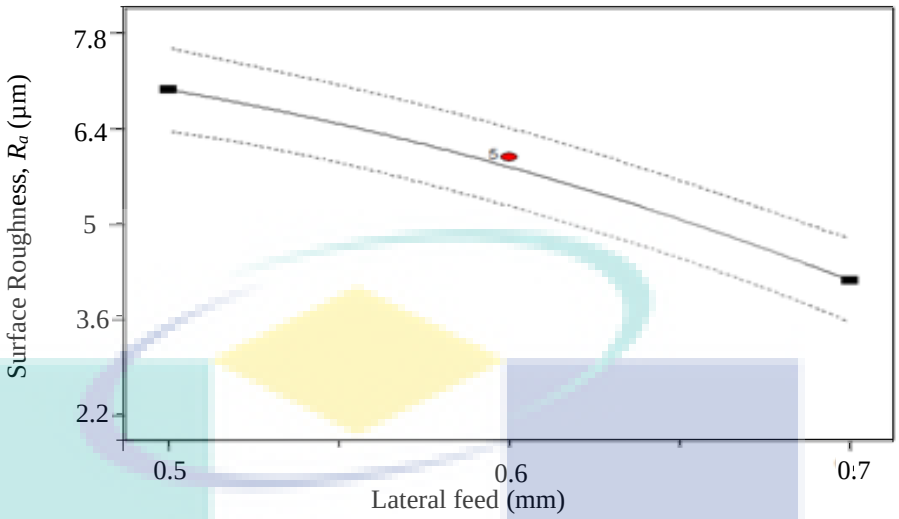

Figure 4-21 Effect of lateral feed on surface roughness minimization

4.4.6 Visual observation – CCD

Figure 4.22 shows visual effect of paint using single pass, traverse rate of 500 mm/min, standoff distance 10 mm at different lateral feed and pressures. Few black area/lines were observed in Figure 4.22 (c), (d), (g) and (h) reflecting that more paints were removed. Paul et al. (1998) found that low lateral feed contributes to more material removal at the centre of previous pass instead on the next spot (at feed away distance from the centre of previous pass) using single pass in machining steel. Low lateral feed allows the jet to interact more with previous machined surface (Paul, Hoogstrate, Luttervelt, & Kals, 1998). Current study employed single pass cleaning with different lateral feed and pressure value. It is interesting to note that, the highest pressure of 36.2 MPa shows more black area compared to low pressure. This indicates that high pressure penetrates more jet particles into the paint rather than removing the surface.

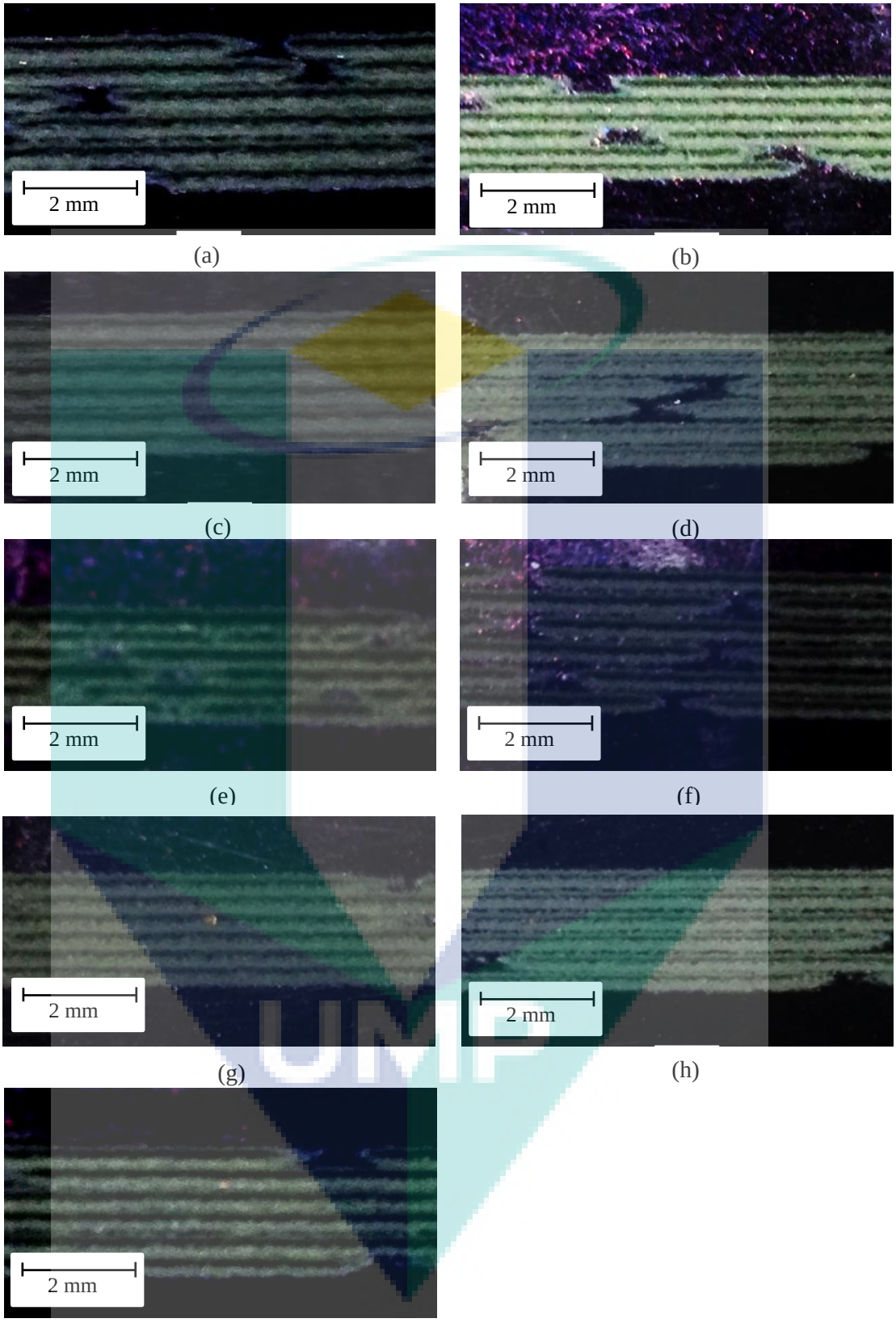

Figure 4-22 Visual effect of paint removal using single pass, traverse rates 500 mm/min , standoff distance 10 mm at different lateral feed and pressures, (a) p = 32.8 MPa, f = 0.6 mm (b) p = 33.6 MPa, f = 0.5 mm (c) p = 34.0 MPa, , f = 0.6 mm (d) p = 33.6 MPa, f = 0.7 mm (e) p = 34.0 MPa, f = 0.4 mm (f) p = 34.0 MPa, f = 0.8 mm (g) p = 35.3 MPa, f = 0.5 mm (h) p = 35.3 MPa, f = 0.7 mm (i) p = 36.2 MPa, f = 0.6 mm

4.4.7 Interaction effects and RSM plot from CCD

Design Expert software (7.0) was used to complete desirability analysis using 'larger the better' desirability function (Rajmohan, 2015). The targets and ranges of input parameters pressure and lateral feed as well as surface roughness were given in Table 4-4. The primary objective of the study is to minimize desirability function by finding the optimal setting. Calculated value of every predicted response was transformed into dimensionless values (d) between 0 and 1 in desirability approach. The value d = 0 shows poor response and d = 1 shows close to criterion response (Rajmohan, 2015). Surface roughness was assigned with the importance of 3.

Table 4-4 Constraints of machine parameters and responses

Parameters	Target	Lower limit	Upper limit	Lower weight	Upper weight	Importance
Pressure	Is in range	4875	5125	1	1	3
Lateral feed	Is in range	0.5	0.7	1	1	3
Surface roughness	minimize	2.204	7.729	1	1	3

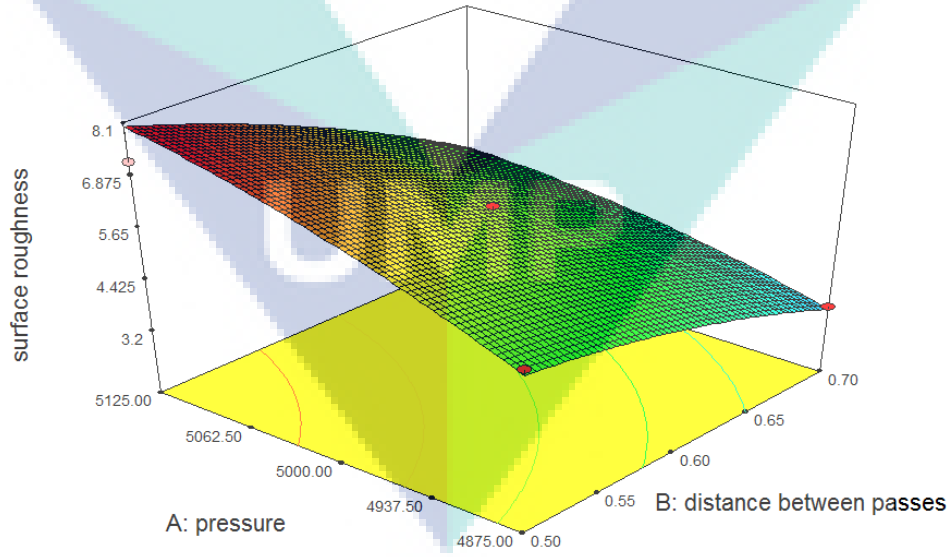

Figure 4-23 3D desirability plot of surface roughness shows the functions of pressure and lateral feed at traverse rate of 500 mm/min, stand-off distance at 10 mm and single cleaning pass.

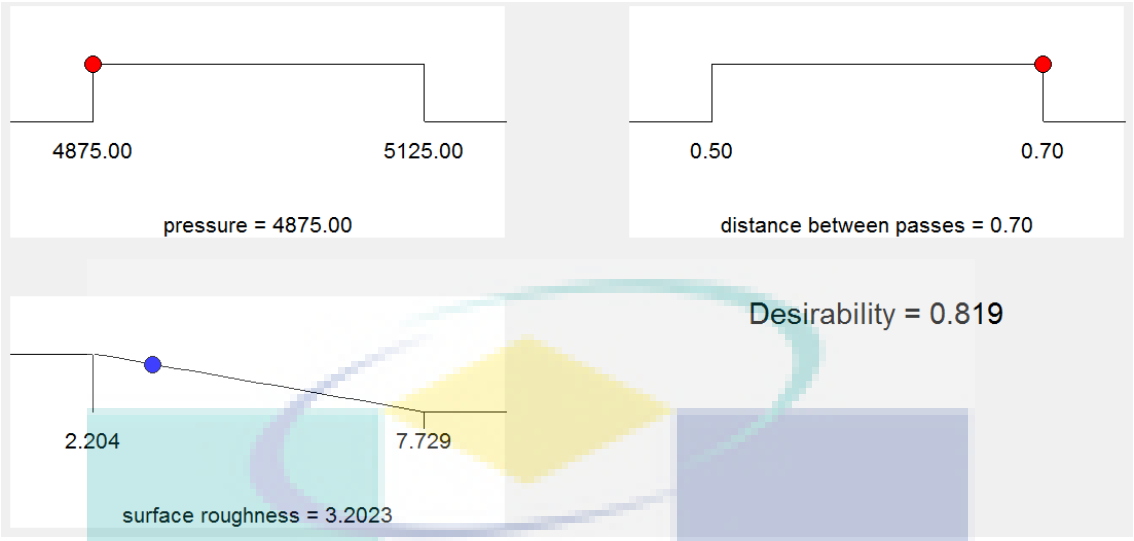

Figure 4-24 Bar graph of surface roughness functions as pressure and lateral feed at traverse rate of 500 mm/min, stand-off distance of 10 mm and single cleaning pass.

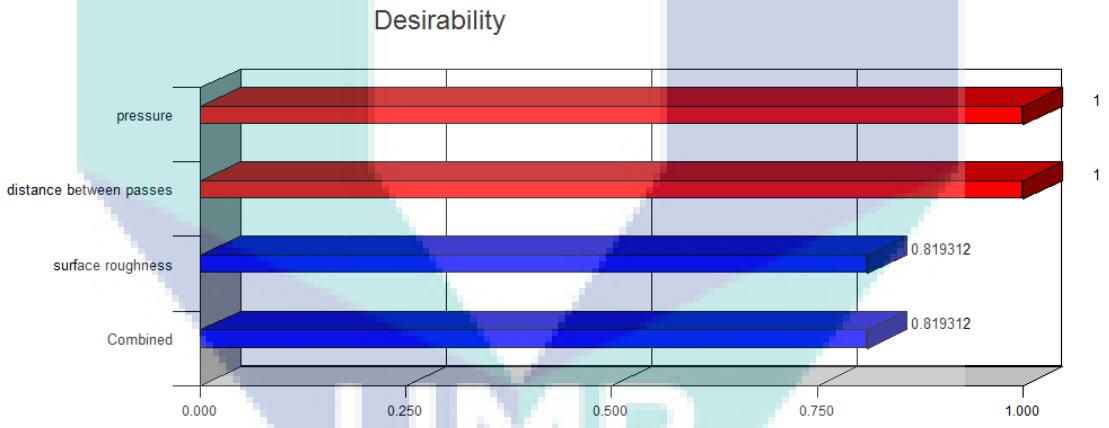

Figure 4-25 Ramp function graph of surface roughness as a function of pressure and lateral feed at traverse rate of 500 mm/min, stand-off distance of 10 mm and single cleaning pass.

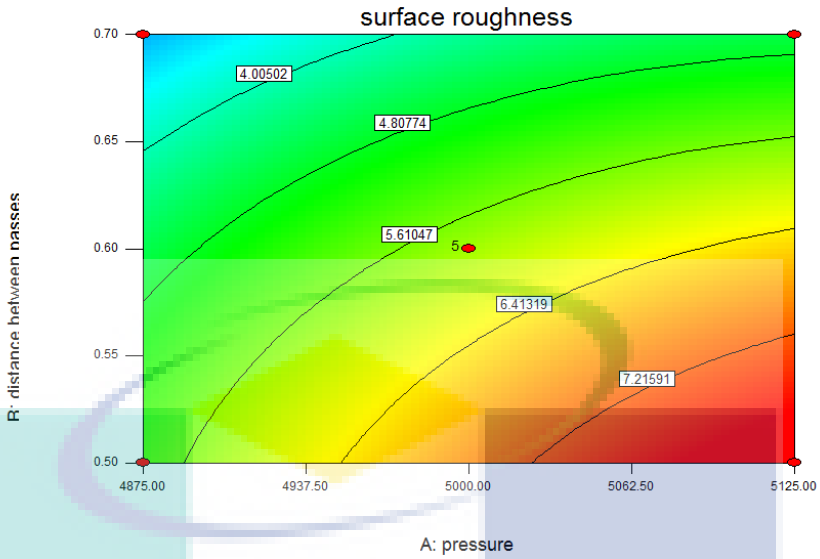

Figure 4-26 Figure contour plots of surface roughness functions as pressure and lateral feed at traverse rate of 500 mm/min, stand-off distance at 10 mm and single cleaning pass.

Figure 4.23 and Figure 4.24 show three dimensional surface desirability plots and optimization bar graph of surface roughness as a function of pressure and lateral feed at traverse rate of 500 mm/min, stand-off distance of 10 mm and single cleaning pass. Optimal solution was derived with the help of point on the ramp graph in Figure 4.25 and Figure 4.26.

4.4.8 Optimization for CCD

Three optimal solutions were randomly selected to check the validity of response surface equation.

Table 4-5 Optimal combination for surface roughness for high desirability

Number	Pressure	Lateral feed	Surface roughness	Desirability	Remarks
1	33.6	0.70	3.20230	0.819	Selected
2	33.6	0.70	3.22004	0.816	
3	33.6	0.70	3.23481	0.813	

In case of cleaning paint, the optimum parameter is defined as parameter that gives the lowest value of surface roughness indicating minimum surface damage. The more the value near to surface roughness of automotive surface substrate which is polypropylene, the best cleaning parameter was obtained. For this automotive part paint

cleaning, optimum value is found in Table 4-5 at 3.20230 µm and this was obtained at the following operative conditions: pressure of 33.6 MPa, traverse rate of 500 mm/min, standoff distance of 10 mm, passes of 1 and lateral feed of 0.7 mm. This parameter was reconfirmed using validation test and prediction error was recalculated to check for error occurrences.

4.5 Validation test

RSM model prediction and experimental test data are given in Table 4-6. It was discovered that the percentage of error is very low. Hence, the developed model is quite acceptable. From the validation test, it was observed that the model prediction is less than 5% of the experimental results value which the percentage is also accepted in other researches (Shanmugam et al., 2019).

Table 4-6 Validation test results

Experiment number	Response Surface Methodology model prediction (Ra)	Experimental results (Ra)	Prediction error (%)
1	3.22555	3.20230	1.04
2	3.24325	3.22004	0.71
3	3.22555	3.23481	0.29

4.5.1 Visual observation from validation test

Figure 4-27 Visual observation of optimum parameter with pressure at 33.6 MPa, traverse rate at 500 mm/min, standoff distance at 10 mm, passes at 1 and lateral feed at 0.7 mm

Figure **4-27** displays visual observation of optimum parameter from the final optimization process with pressure of 33.6 MPa, traverse rate of 500 mm/min, standoff distance of 10 mm, number of cleaning passes of 1 and lateral feed of 0.7 mm. It was observed that almost all paint was removed at the cleaning area except some amount of paint at the small gap between consecutive cleaning passes. This is proven by the existence of black area at the gap which reflects some paint left. For more accurate observation, a 3D image surface structural test was performed.

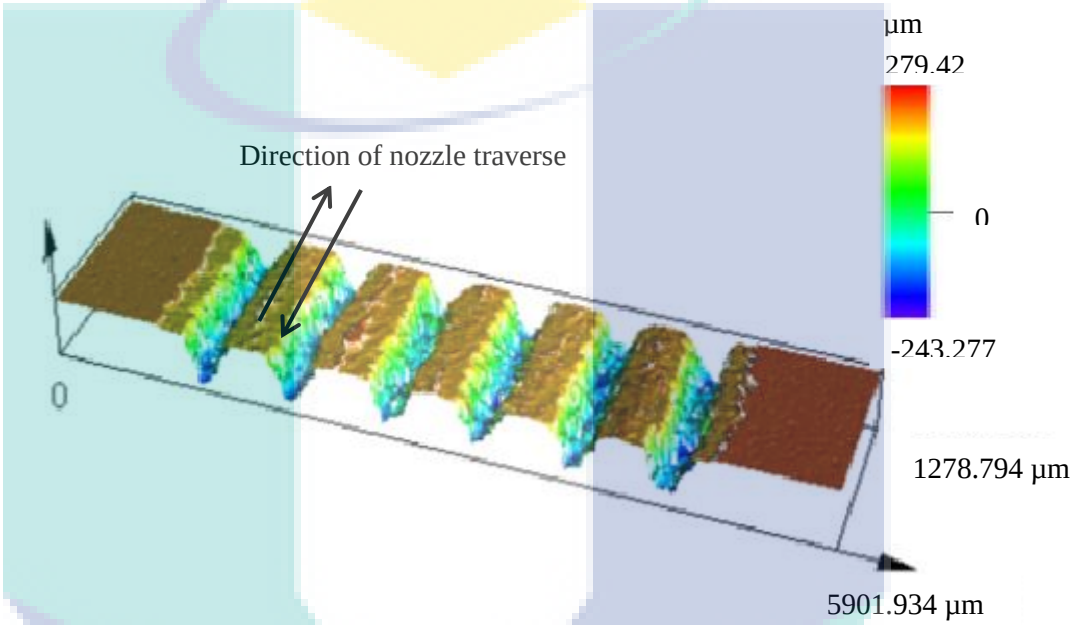

Figure 4-28 3D image of surface structures with optimum parameter for pressure at 33.6 MPa, traverse rate at 500 mm/min, standoff distance at 10 mm, number of passes at 1 and lateral feed at 0.7 mm

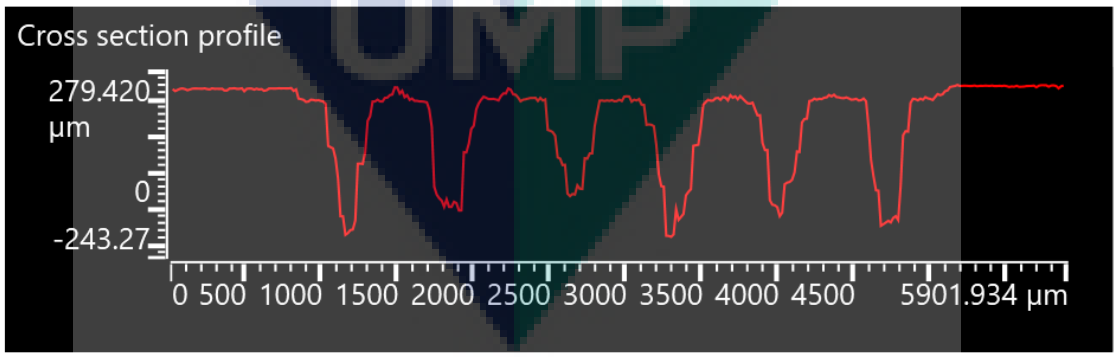

Figure 4-29 Cross section profile of optimum parameter with pressure at 33.6 MPa, traverse rate at 500 mm/min, standoff distance at 10 mm, number passes of 1 and lateral feed at 0.7 mm

Figure 4-28 displays 3D image of surface structures with optimum parameter from final optimization process including pressure at 33.6 MPa, traverse rate at 500

mm/min, standoff distance at 10 mm, cleaning passes of 1 and lateral feed at 0.7 mm; whereas Figure 4-29 shows its cross sectional profile. High erosion material is wavy–shaped in the image with valley-to-peak values are in a range of 279.42 µm to -243.277µm. It was observed in Figure 4-29 that the erosion width is almost constant where the depth is low in the middle of cross-sectional profile.

4.6 Summary

From this section, the analysis of the surface roughness of the cleaned surface was analysed by using RSM. The optimum waterjet parameter to achieve maximum paint erosion with minimum surface damage was obtained.

CHAPTER 5

CONCLUSIONS AND RECOMMENDATIONS

5.1 Conclusions

The main objective of the study is to determine optimum waterjet parameters combination of waterjet parameters to remove automotive paint using response surface methodology (RSM). Based on the experimental results, analysis of variance (ANOVA), confirmation test results and mathematical models, subsequent conclusions are made for effective automotive paint cleaning by plain waterjet process:

1. Plain waterjet cleaning (by imparting new method with number of cleaning passes and lateral feed) is a realistic method to successfully remove automotive paint with acceptable quality namely surface roughness. It is vital to have proper selection of plain waterjet cleaning parameter to certify optimum quality characteristics.

2. Lateral feed and pressure are the most significant factors influencing surface roughness as can be seen from the pareto chart; followed by number of cleaning passes, traverse rate and standoff distance.

3. The suggested optimal parametric combination for better surface finish is under the condition of waterjet pressure at 33.6 MPa, traverse rate at 500 mm/min, standoff distance at 10 mm, number of cleaning passes of 1 and lateral feed at 0.7 mm.

4. Mathematical model for surface roughness was developed based on linear regression analysis technique. The model successfully predicted surface roughness of plain waterjet machine for automotive paint cleaning within the

study's limitation. It serves as machining parameters which includes waterjet pressure, traverse rate, standoff distance, number of cleaning passes and lateral feed.

5. It is a challenge to obtain effective automotive paint cleaning method using non-conventional machining process, especially plain waterjet. RSM based on analysis for investigating effect of plain waterjet parameters provides efficient procedures to real-world operators. Therefore, it is obvious that numerous studies based on RSM, qualitative modelling and experimental results as found in current study are valuable for scrutinizing the effect of various process parameters in attaining appropriate control over cleaning efficiency.

5.2 Recommendations

The following recommendations for further studies on waterjet for automotive paint cleaning should be considered:

1. Other waterjet parameters such as water-orifice diameter, nozzle diameter and attack angle should be considered to investigate their influence on cleaning quality of automotive paint.

2. For response or assessment purpose, other cleaning qualities or surface quality (apart from current study) should be analysed such as paint removal rate, width of cleaning etcetera to determine the effect of waterjet on the response.

3. The material in this study is only one type and one paint colour. There are other types and colours of automotive paint which can be used to study the response on waterjet paint cleaning. In addition, abrasive waterjet technique should also be further studied.

REFERENCES

Adalarasan Ramalingam, S. M. (2015). Application of Response Surface Methodology in Abrasive Waterjet Machining of High Speed Steel. *International Journal of Applied Engineering Research*, *10*(December).

Akafuah, N. K., Poozesh, S., Salaimeh, A., Patrick, G., & Lawler, K. (2016). Evolution of the Automotive Body Coating Process — A Review. https://doi.org/10.3390/coatings6020024

Andriani, S. E., Catalano, I. M., Daurelio, G., & Albanese, A. (2007). Marker and pen graffiti cleaning on diverse calcareous stones by different laser techniques. *Proc. SPIE 6346, XVI International Symposium on Gas Flow, Chemical Lasers, and High-Power Lasers.*, *6346*(April), 634636–1/10.

Anglani, F., Barry, J., Dekkers, W., K. S. (2017). CFD modelling of a water-jet cleaning process for concentrated solar thermal (CST) systems, (February).

Aydin, G., Karakurt, I., & Aydiner, K. (2011). An investigation on surface roughness of granite machined by abrasive waterjet, *34*(4), 985–992.

Azhari, A., & Schindler, C. (2012). Improving surface hardness of austenitic stainless steel using waterjet peening process, 1035–1046.

Azhari, A., Schindler, C., & Li, B. (2013). Effect of waterjet peening on aluminum alloy 5005, 785–795.

Babu, M. Naresh, N. M. (2014). Investigation on Surface Roughness in Abrasive Water Jet Machining by the Response Surface Method. *Material and Manufacturing Process*, (August), 37–41.

Badgujar, P. P., & Rathi, M. G. (2014). Analysis of surface roughness in abrasive waterjet cutting of stainless steel. *International Journal of Engineering Research and Technology*, *3*(6), 209–212.

Balasubramaniam, R., Krishnan, J., Ramakrishnan, N., Bitter, J. G. a. G. A., Blind, J. B. Æ. P., Communication, S., … Zhao, J. (1963). Characteristics Study of Flexible Magnetic Abrasive in Abrasive Jet Machining. *Procedia CIRP*, *6*(1), 169–190.

Barletta, M., Gisario, A., & Tagliaferri, V. (2006). Advance in paint stripping from aluminium substrates, *173*(December 2004), 232–239.

Careddu, N., & Akkoyun, O. (2016). An investigation on the efficiency of water-jet technology for graffiti cleaning. *Journal of Cultural Heritage*, *19*, 426–434.

Carvalhão, M., & Dionísio, A. (2015). Evaluation of mechanical soft-abrasive blasting and chemical cleaning methods on alkyd-paint graffiti made on calcareous stones. *Journal of Cultural Heritage*, *16*(4), 579–590.

Chapman, S. (2000). Laser technology for graffiti removal. *Journal of Cultural Heritage*, *1*, 75–78.

Chillman, A., Ramulu, M., & Hashish, M. (2016). Waterjet and Water-Air Jet Surface Processing of a Titanium Alloy : A Parametric Evaluation, 1–10.

Chizari, M., Barrett, L. M., & Al-Hassani, S. T. S. (2009). An explicit numerical modelling of the water jet tube forming. *Computational Materials Science*, *45*(2), 378–384.

Costela, A., García-Moreno, I., Gómez, C., Caballero, O., & Sastre, R. (2003). Cleaning graffitis on urban buildings by use of second and third harmonic wavelength of a Nd:YAG laser: A comparative study. *Applied Surface Science*, *207*(1–4), 86–99.

Fiorucci, M. P., Lopez, A. J., Ramil, A., Pozo, S., & Rivas, T. (2013). Optimization of graffiti removal on natural stone by means of high repetition rate UV laser. *Applied Surface Science*, *278*, 268–272.

Fiorucci, M. P., López, A. J., Ramil, A., Pozo, S., & Rivas, T. (2013). Optimization of graffiti removal on natural stone by means of high repetition rate UV laser. *Applied Surface Science*, *278*, 268–272.

Folkes, J. (2009a). Journal of Materials Processing Technology Waterjet — An innovative tool for manufacturing, *209*, 6181–6189.

Folkes, J. (2009b). Waterjet-An innovative tool for manufacturing. *Journal of Materials Processing Technology*, *209*(20), 6181–6189.

Gomes, V., Dionísio, A., & Pozo-Antonio, J. S. (2017). Conservation strategies against graffiti vandalism on Cultural Heritage stones: Protective coatings and cleaning methods. *Progress in Organic Coatings*, *113*(August), 90–109.

Gomes, V., Dionísio, A., Pozo-antonio, J. S., Rivas, T., & Ramil, A. (2018). Mechanical and laser cleaning of spray graffiti paints on a granite subjected to a SO 2 -rich atmosphere. *Construction and Building Materials*, *188*, 621–632.

Hloch, S., Fabian, S., & Rim, M. (2008). Design of experiments applied on abrasive waterjet factors sensitivity identification, (2), 49–57.

Khairul, M., Abdul, A., Noor, M., & Suhaimi, M. (2018). A review of incorporating Nd : YAG laser cleaning principal in automotive industry. *Journal of Radiation Research and Applied Sciences*, *11*(4), 393–402.

Kovacevic, M. and. (1998). Principles of Abrasive Water Jet Machining. *Springer London*.

Kovacevic, R. (n.d.). Surface Texture in Abrasive Waterjet Cutting, 32–40.

Lee, A., Chaibakhsh, N., Basyaruddin, M., Rahman, A., Basri, M., & Tejo, B. A. (2010). Optimized enzymatic synthesis of levulinate ester in solvent-free system. *Industrial Crops & Products*, *32*(3), 246–251.

Mabrouki, T., & Raissi, K. (2002). Stripping process modelling : interaction between a moving waterjet and coated target, *42*, 1247–1258.

Matsui, I., Onda, A., Shinozaki, S., Kyo, E., Nagai, K., & Yuasa, N. (2006). Method of Removing Graffiti from Surface of Concrete. *Key Engineering Materials*, *302*–

303(January 2006), 363–370.

Mazzinghi, P., & Margheri, F. (2003a). A short pulse, free running, Nd: YAG laser for the cleaning of stone cultural heritage. *Optics and Lasers in Engineering*, *39*(2), 191–202.

Mazzinghi, P., & Margheri, F. (2003b). A short pulse, free running, Nd:YAG laser for the cleaning of stone cultural heritage. *Optics and Lasers in Engineering*, *39*(2), 191–202.

Miles, P. (2013). Rz : A Better measurement of abrasive waterjet cut surface finishes.

Mohammed, H., Iqbal, A., & Hashemipour, M. (2014). Dimensional accuracy and strength comparison in hole making of GFRP composite using Co 2 laser and abrasive water jet technologies, *21*(April), 189–199.

Moura, A., Flores-Colen, I., de Brito, J., & Dionisio, A. (2017). Study of the cleaning effectiveness of limestone and lime-based mortar substrates protected with anti-graffiti products. *Journal of Cultural Heritage*, *24*, 31–44.

Murugan, M., Gebremariam, M. A., Hamedon, Z., & Azhari, A. (2018). Performance Analysis of Abrasive Waterjet Machining Process at Low Pressure Performance Analysis of Abrasive Waterjet Machining Process at Low Pressure, 0–6.

Oka, Y. I., Mihara, S., & Miyata, H. (2007). Effective parameters for erosion caused by water droplet impingement and applications to surface treatment technology, *263*, 386–394.

Ortiz, P., Antúnez, V., Ortiz, R., Martín, J. M., Gómez, M. A., Hortal, A. R., & Martínez-Haya, B. (2013). Comparative study of pulsed laser cleaning applied to weathered marble surfaces. *Applied Surface Science*, *283*, 193–201.

Pal, V. K., & Choudhury, S. K. (2014). Application of pure waterjet machining for improving surface finish of parts fabricated by abrasive waterjet machining, 1–6.

Paul, S., Hoogstrate, A. M., Luttervelt, C. A. Van, & Kals, H. J. J. (1998). An experimental investigation of rectangular pocket milling with abrasive water jet, *73*, 179–188.

Penide, J., Quintero, F., Riveiro, A., Sánchez-Castillo, A., Comesaña, R., Del Val, J., … Pou, J. (2013). Removal of graffiti from quarry stone by high power diode laser. *Optics and Lasers in Engineering*, *51*(4), 364–370.

Pozo-Antonio, J. S., Rivas, T., Fiorucci, M. P., L??pez, A. J., & Ramil, A. (2016). Effectiveness and harmfulness evaluation of graffiti cleaning by mechanical, chemical and laser procedures on granite. *Microchemical Journal*, *125*, 1–9.

Pozo-Antonio, J. S., Rivas, T., Fiorucci, M. P., López, A. J., & Ramil, A. (2016). Effectiveness and harmfulness evaluation of graffiti cleaning by mechanical, chemical and laser procedures on granite. *Microchemical Journal*, *125*, 1–9.

Radovanovi, M. (2017). Investigation on surface roughness of carbon steel machined by abrasive waterjet using taguchi method, (December 2014).

Rajmohan, M. S. R. A. M. (2015). Experimental Modelling and Analysis in Abrasive Waterjet Cutting of Ceramic Tiles Using Grey-Based Response Surface, 3299–3300.

Ramil, A., Pozo-Antonio, J. S., Fiorucci, M. P., López, A. J., & Rivas, T. (2017). Detection of the optimal laser fluence ranges to clean graffiti on silicates. *Construction and Building Materials*, *148*, 122–130.

Rate, F., Flow, A. M., & Bamboo, R. (2015). com Effect of Pressure, Feed Rate, and Abrasive Mass Flow Rate on Water Jet Cutting Efficiency When Cutting Recombinant Bamboo, *10*(2011), 499–509.

Rivas, T., Pozo, S., Fiorucci, M. P., Lopez, A. J., & Ramil, A. (2012). Nd:YVO4 laser removal of graffiti from granite. Influence of paint and rock properties on cleaning efficacy. *Applied Surface Science*, *263*, 563–572.

Rivero, A., Artaza, T., Lamikiz, A., Alberdi, A., Rivero, A., Artaza, T., & Lamikiz, A. (2017). Analysis of Alloy 718 surfaces milled by abrasive waterjet and post- Analysis of Alloy surfaces milled by abrasive waterjet plain waterjet technology processed by plain waterjet technology Costing models for A . capacity optimization in Industry between u.

Samolik, S., Walczak, M., Plotek, M., Sarzynski, A., Pluska, I., Marczak, J., … Sarzynski, A. (2015). Investigation into the removal of graffiti on mineral supports : Comparison of nano-second Nd : YAG laser cleaning with traditional mechanical and chemical methods Papers from the Tenth Conference on LASERS IN THE CONSERVATION OF ARTWORKS American University of Sharjah Sharjah , United Arab Emirates Editors Abdelrazek Elnaggar Austin Nevin Marta Castillejo Matija Strlič, *3630*(May 2017).

Sanjeevan, P., Klemm, A. J., & Klemm, P. (2007). Removal of graffiti from the mortar by using Q-switched Nd:YAG laser. *Applied Surface Science*, *253*(20), 8543–8553.

Sanmartín, P., Cappitelli, F., & Mitchell, R. (2014). Current methods of graffiti removal: A review. *Construction and Building Materials*, *71*, 363–374.

Selvan, C. P., & Raju, M. S. (2012). Analysis of surface roughness in abrasive waterjet cutting of cast iron, *1*(3), 174–182.

Shanmugam, A., Krishnamurthy, K., Mohanraj, T., Shanmugam, A., Krishnamurthy, K., Mohanraj, T., & Review, S. (2019). Experimental study of surface roughness and taper angle in abrasive water jet machining of 7075 Aluminium composite using response surface methodology.

Tambe, P. B. (2008). Optimisation of surface finish in abrasive water jet cutting of Kevlar composites using hybrid Taguchi and response surface method Tauseef Uddin Siddiqui and Mukul Shukla *, *3*, 382–402.

Tanmay Tiwari, Saket Sourabh, Akash Nag, Amit Rai Dixit, A. M., & Alok Kumar Das, Niladri Mandal, A. K. S. (2018). Parametric investigation on abrasive waterjet machining of alumina ceramic using response surface methodology Parametric investigation on abrasive waterjet machining of alumina ceramic using response surface methodology, 0–7.

Teimourian, H., Shabgard, M. R., & Momber, A. W. (2010). Progress in Organic Coatings De-painting with high-speed water jets : Paint removal process and substrate surface roughness. *Progress in Organic Coatings*, *69*(4), 455–462.

Vergès-Belmin, V., Wiedemann, G., Weber, L., Cooper, M., Crump, D., & Gouerne, R. (2003). A review of health hazards linked to the use of lasers for stone cleaning. *Journal of Cultural Heritage*, *4*, 33–37.

Vorburger, T. V, Renegar, T. B., Zheng, A. X., Song, J., Soons, J. A., & Silver, R. M. (2009). NIST SURFACE ROUGHNESS AND STEP HEIGHT CALIBRATIONS , Measurement Conditions and Sources of Uncertainty, 1–9.

Wang, J., & Guo, D. M. (2003). The cutting performance in multipass abrasive waterjet machining of industrial ceramics, *133*, 1–7.

Wang, J., Kuriyagawa, T., & Huang, C. Z. (2003). An experimental study to enhance the cutting performance in abrasive waterjet machining, *7*, 1–15.

Weaver, M. E. (1832). Removing Graffiti from Historic Masonry.

Yadav, G. S., & Singh, B. K. (2016). Effect of Process Parameter in Abrasive Water Jet Cutting Using Response Surface Method, 981–985.

Yue, Z., Huang, C., & Zhu, H. (2014). Optimization of machining parameters in the abrasive waterjet turning of alumina ceramic based on the response surface methodology, 2107–2114.

Zhang, H., & Chen, M. (2015). Theoretical Analysis and Experimental Study on the Coating Removal from Passenger-Vehicle Plastics for Recycling by Using Water Jet Technology, *67*(11), 2714–2726.

LIST OF PUBLICATION

[1] Nawi M.N.M., Husin H., Gebremariam M.A., Azhari A. (2020) Investigation on the Effect of Multiple Passes in Plain Waterjet Cleaning of Paint. In iMEC-APCOMS 2019. iMEC-APCOMS 2019. Lecture Notes in Mechanical Engineering. Springer, Singapore, pp. 537-543.

[2] Husin H., Nawi M.N.M., Gebremariam M.A., Azhari A. (2020) Investigation on the Effect of Abrasive Waterjet Parameter on Machining Stainless Steel. In iMEC-APCOMS 2019. iMEC-APCOMS 2019. Lecture Notes in Mechanical Engineering. Springer, Singapore, pp. 544-549.

[3] Husin S.H., Helmi N.M., Fatchurrohman N., Gebremariam M.A., Azhari A. (2020) Effect of Delamination in Drilling of Natural Fibre-Reinforced Composite. In: Osman Zahid M., Abd. Aziz R., Yusoff A., Mat Yahya N., Abdul Aziz F., Yazid Abu M. (eds) iMEC-APCOMS 2019. iMEC-APCOMS 2019. Lecture Notes in Mechanical Engineering. Springer, Singapore, pp. 472-477.

Investigation on the Effect of Multiple Passes in Plain Waterjet Cleaning of Paint

Mohd Nazir Mat Nawi[1,2(✉)], Hafiz Husin[1,2], M. A. Gebremariam[1], and Azmir Azhari[1]

[1] Faculty of Manufacturing Engineering, Universiti Malaysia Pahang, 26600 Pekan, Malaysia
mhd_nazir@yahoo.com
[2] Centre for Foundation Studies, International Islamic University Malaysia, 26300 Gambang, Malaysia

Abstract. Paint removal process in automotive coating is widely used in vehicle component recycling industry. The need of utilization and recycling the automotive component without producing secondary pollution from the paint removal process is recently become a major concern globally. Water jet cleaning is a new method for paint removal and getting recognition because of environmental friendly and it is better than mechanical cleaning such as sand blasting, brushing with water, hydropneumatic cleaning, controlled dry sanding, low pressure water projection and low pressure water spray. The present study focuses on the investigation of effect of multiple passes in plain water jet cleaning on paint removal process. A new method of multiple passes treatment is applied in plain water jet cleaning to access its effect on surface roughness and paint removal rate. It was found that, with increasing of number of passes, the surface roughness and paint removal rate is slightly increase. It is also found that the increase in water jet pressure will increase the surface roughness and paint removal rate. This is probably because increasing pressure will leads to more energy to remove the paint. It is found also that the increase in traverse rate increase the surface roughness and decrease paint removal rate. Based on the present study, it is a high prospect to apply multiple passes of paint removal using plain water jet in automotive industry.

Keywords: Paint removal · Waterjet cleaning · Multiple jet passes

1 Introduction

A removal process of deposits, contaminates and coating materials from the substrates of parts or manufacturing product is defined as a fundamental in industrial technology. Applications of this technique involve in various fields including automotive paint removal industry. Paints are resulting from pigments (such as iron oxide, carbon black or aluminium among others) combined with synthetic resins (thermoplastics or thermostable) which permit the bonding between the paint and the substrates [1].

In paint removal, the main objective is high cleaning efficiency and paint erosion with minimum substrate damage. The current study focuses on cleaning method mostly using laser. Cleaning by laser is found to cause damage to the substrate, alteration of

© Springer Nature Singapore Pte Ltd. 2020
M. N. Osman Zahid et al. (Eds.): iMEC-APCOMS 2019, LNME, pp. 537–543, 2020.
https://doi.org/10.1007/978-981-15-0950-6_82

mhd_nazir@yahoo.com

Investigation on the Effect of Abrasive Waterjet Parameter on Machining Stainless Steel

Hafiz Husin[1,2](✉), Mohd Nazir Mat Nawi[1,2], M. A. Gebremariam[1], and Azmir Azhari[1]

[1] Faculty of Manufacturing Engineering, Universiti Malaysia Pahang, 26600 Pekan, Malaysia
hafidzukn@yahoo.com

[2] Centre for Foundation Studies, International Islamic University Malaysia, 26300 Gambang, Malaysia

Abstract. Abrasive waterjet machining (AWJM) can perform various machining operations on almost any material including hard to machine materials. However, performance of a process depends on the chosen set of parameters. AWJM has major parameters such as traverse rate, water pressure, standoff distance and abrasive flowrate that will affect its performance. The present study investigates the effects of AWJM parameters (i.e. traverse rate, water pressure and standoff distance) on the width, depth and roughness of a channel produced at the surface of stainless steel. The results showed that by reducing the standoff distance and water pressure, the width of the channel was also reduced. For channel depth, increasing traverse rate produced a shallower channel depth. In contrast, increasing the water pressure produced a deeper channel depth. The surface roughness of the channel showed significant improvement by reducing the water pressure at a lower traverse speed and standoff distance. A proper selection of parameters is required in order to produce a suitable channel during AWJM surface texturing process.

Keywords: Abrasive waterjet machining · Waterjet channeling

1 Introduction

This paper discusses the effects of abrasive waterjet machining of parameter on surface texturing on stainless steel. Waterjet either in plain form or mixed with abrasive can perform various machining operation on almost any material including hard to machine material. The application is endless and it is nontraditional machining method that has been chosen by manufacturers due to its flexibility and reliability [1]. Performance of any process depends on the parameter chosen. AWJM has major parameter such as traverse rate, water pressure, standoff distance, abrasive flowrate and abrasive particle size that affects the performance of the AWJM [2]. AWJM has no machine vibration or

© Springer Nature Singapore Pte Ltd. 2020
M. N. Osman Zahid et al. (Eds.): iMEC-APCOMS 2019, LNME, pp. 544–549, 2020.
https://doi.org/10.1007/978-981-15-0950-6_83
mhd_nazir@yahoo.com

Effect of Delamination in Drilling of Natural Fibre-Reinforced Composite

Suraya Hamirudin Husin, Nurul Mohd Helmi, Nanang Fatchurrohman, Mebrahitom A. Gebremariam, and Azmir Azhari(✉)

Faculty of Manufacturing and Mechatronics Engineering Technology, Universiti Malaysia Pahang, 26600 Pekan, Malaysia
azmi r@ump. edu. my

Abstract. The use of natural fibre-reinforced composites is continuously getting more attention worldwide mainly due to their environmental friendliness. The present work investigates the effect of drilling parameters namely spindle speed and feedrate on the delamination damage of Kenaf fibre-reinforced composite laminates. Two different laminate thicknesses were fabricated (i.e. 4 and 6 mm). It was found that the spindle speed did not significantly affect the delamination damage. Whereas, increasing the feedrate resulted in a higher delamination factor possibly because of a higher thrust force. Meanwhile, the different in laminate thicknesses did not notably influence the delamination damage during the drilling process. The results of the present work are useful to be used for future reference in the study on the drilling of natural fibre-reinforced composite.

Keywords: Natural fibre reinforced composite · Drilling process · Push-out delamination

1 Introduction

Reinforced plastics composite material is a combination of various sources of reinforcement materials and plastics which acts as a binder. As a result, it can withstand a stronger load as the strength and other properties are improved. Reinforcements are used to provide the strength and rigidity at a lower cost. In recent years, there is a tendency to use composite materials in many industries due to its various advantages. However, majority of reinforcement materials or fibres are made from non-biodegradable materials. Lately, there is a huge interest of using natural fibre-reinforced composites (NFRC) due to the environmental and sustainability aspects of engineering materials. NFRC also offer numerous benefits which includes low cost, biodegradability, eco-friendly nature and relatively good mechanical properties [1].

Amongst various machining processes, drilling is a commonly employed technique in industry because of the requirement to assemble components in mechanical pieces and structures. The drilling of composite laminates is significantly affected by the tendency of these materials to delaminate under the action of drilling forces (thrust force) which may result in fibre pull-out and thermal damages especially the polymeric

© Springer Nature Singapore Pte Ltd. 2020
M. N. Osman Zahid et al. (Eds.): iMEC-APCOMS 2019, LNME, pp. 472–477, 2020.
https://doi.org/10.1007/978-981-15-0950-6_72

mhd_nazir@yahoo.com